Geoscience Frontiers 13 (2022) 101372

HOSTED BY

Contents lists available at ScienceDirect

Geoscience Frontiers

journal homepage: www.elsevier.com/locate/gsf

Research Paper

Paleo- and Mesoarchean TTG-sanukitoid to high-K granite cycles in the southern São Francisco craton, SE Brazil

Claudio de Morisson Valeriano [a,*], Caio Vinicius Gabrig Turbay [b], Henrique Bruno [a,c], Antonio Simonetti [d], Monica Heilbron [a], Samuel Moreira Bersan [a], Rob Strachan [c]

[a] Universidade do Estado do Rio de Janeiro, Faculdade de Geologia, Rua São Francisco Xavier 524/4006-B, Maracanã, Rio de Janeiro, Brazil
[b] Universidade Federal do Sul da Bahia, Centro de Formação em Ciências Ambientais, Porto Seguro, Bahia, Brazil
[c] University of Portsmouth, School of Environment, Geography and Geosciences, Burnaby Building, Burnaby Road, Portsmouth PO1 3QL, United Kingdom
[d] University of Notre Dame, Department of Civil and Environmental Engineering and Earth Sciences, 46556, United States

ARTICLE INFO

Article history:
Received 14 June 2021
Revised 19 January 2022
Accepted 15 February 2022
Available online 18 February 2022

Keywords:
Crustal evolution
Sm–Nd
Lu–Hf
LA-ICPMS zircon U–Pb

ABSTRACT

The generation of the continental crust is widely accepted to have taken place predominantly in the Archean, when TTG magmatism associated with greenstone-belt supracrustal succession development was typically followed by emplacement of high-K granites before crustal stabilization. This study focuses on the Campos Gerais complex (CGC), which is an Archean granite-greenstone belt lithological association in a tectonic window located in the southwesternmost portion of the São Francisco craton (SFC). The CGC is an important segment of Paleo- to Mesoarchean continental crust to be integrated into paleogeographic reconstructions prior to the transition into the Paleoproterozoic. This investigation reports field relationships, 28 major and trace element compositions, U–Pb (zircon) geochronological results, and Hf and Sm–Nd isotope data for orthogneiss and amphibolite samples. The results indicate that the CGC records a complex Archean crustal evolution, where voluminous 2.97 Ga TTG tonalites and trondhjemites ($\varepsilon_{Nd}(t)$ = − 4.7; T_{DM} = 3.24 Ga) were followed by 2.89 Ga sanukitoid tonalite production ($\varepsilon_{Nd}(t)$ = − 1.9; T_{DM} = 3.02 Ga), broadly coeval with the development of the Fortaleza de Minas and Pitangui greenstone-belts. These events are interpreted to represent the initial stage of an important subduction-accretion tectonic cycle, which ended with the emplacement of 2.82–2.81 Ga high-K leucogranites and migmatization of the TTG-sanukitoid crust, with hybrid and two-mica, peraluminous compositions ($\varepsilon_{Nd}(t)$ = − 8.0 to − 8.6; T_{DM} = 3.57 – 3.34 Ga). The presence of inherited zircons with $^{207}Pb/^{206}Pb$ ages of 3.08 Ga, 3.29 Ga, 3.55 Ga and 3.62 Ga indicates that the Mesoarchean tectonic processes involved reworking of Meso- to Eo-archean crust. Renewed TTG magmatism took place at ca. 2.77 Ga represented by juvenile tonalite stocks ($\varepsilon_{Nd}(t)$ = +1.0 to − 1.5; T_{DM} = 2.80 – 2.88 Ga) which intrude the TTG-greenstone belt association. Crustal stabilization was attained by 2.67 Ga, allowing for the emplacement of within-plate tholeiitic amphibolites ($\varepsilon_{Nd}(t)$ = − 3.1; T_{DM} = 2.87 Ga). The CGC shows important tectonic diachronism with respect to other Archean terrains in the southern São Francisco craton, including an independent Meso- to Neoarchean crustal evolution.

1. Introduction

Archean terranes are windows into the primordial tectonic mechanisms operating on Earth and represent relics of the first stable continents that survived recycling through younger collisional processes (Mulder et al., 2021). The nucleation of the first continental blocks in early Earth seems to be dominated by the development of widespread TTG (tonalite-trondhjemite-granodiorite) complexes, associated with supracrustal associations (Moyen and Laurent, 2018). TTG magmatism, coeval with, or followed by, sanukitoid rocks, have been widely recognized in Archean cratons worldwide (e.g., Heilimo et al., 2010; Laurent et al., 2014; Bruno et al., 2020). The typical oval dome geometry of Archean TTG complexes, separated by keels of supracrustal ("greenstone belt")

Abbreviations: Sm-Nd, Samarium-Neodymium; Lu-Hf, Lutetium-Hafnium; LA-ICPMS, Laser Ablation Inductively Coupled Mass Spectrometry; U-Pb, Uranium-Lead.

* Corresponding author.
E-mail address: valeriano.claudio@gmail.com (C. de Morisson Valeriano).

https://doi.org/10.1016/j.gsf.2022.101372
1674-9871/

associations, has given rise to geodynamic models where continental nucleation took place in intraplate environments through predominantly vertical, gravity induced tectonics (Bedard, 2006, 2018).

The transition of TTG to sanukitoid magmatism is commonly interpreted as the result of partial melting of respectively subducted oceanic crust and overlying mantle wedge, in a subduction-like tectonic setting (Bruno et al., 2020; Heilimo et al., 2010; Laurent et al., 2014; Moyen and Laurent, 2018). However, a debated topic in geodynamics is whether subduction as we know today would have been stable in Archean times due to higher mantle temperatures, which is commonly argued as an impediment to stable subduction processes (Gerya, 2014). Smithies et al. (2021) presented an entirely intracrustal differentiation process for the TTG-sanukitoid rock association, based on the geology of the Paleoarchean Pilbara Craton, Australia, which displays a conspicuous dome-and-keel structure (François et al., 2014; Wiemer et al., 2018). In their model, hydrated greenstone-belt keels would drip in a gravity-driven crustal convective overturn, releasing fluids and hydrated partial melts, to result in metasomatically enriched lithospheric mantle as the source for the sanukitoid magmas. However, as suggested by the numerical models from Roman and Arndt (2020), sagduction-like dripping is not a plausible mechanism for transporting hydrated crustal material into mantle depths, suggesting that subduction-related horizontal tectonic process was the main mechanism for generation of Archean granitoids. The most commonly proposed mechanism for the origin of sanukitoid magma, a product of mixed crustal and mantle reservoirs, is the interaction between metasomatized mantle and crust-derived magmas in which the opening of a mantle wedge through subduction would be a suitable process to enrich the asthenospheric mantle with crustal components, as is observed today (Heilimo et al., 2010; Laurent et al., 2014; Rajesh et al., 2018).

The geochemical characteristics of such subduction-related magmas, such as Nb, Ta, P and Ti depletion relative to the composition of the mantle, are in a uniformitarian way interpreted as the result of the interaction between percolating fluids derived from progressive dehydration of subducted oceanic slab with the overlying modified mantle wedge (Pearce, 1982). The Archean subduction-collision tectonic models are based on global findings of TTG-sanukitoid magmatic associations pre-dating high-K peraluminous granites and migmatization of previously formed continental crust, which are interpreted as the temporal markers of collisional processes associated with regional metamorphic events, followed by regional cooling and tectonic stabilization (Halla, 2005; Larionova et al., 2007; Jiang et al., 2016; Windley et al., 2020). Such a succession of tectonic processes is described here in the São Francisco craton (SFC; Fig. 1), the South American portion of the larger São-Francisco-Congo Paleocontinent, regarded as having been essentially preserved from the peripheral Neoproterozoic orogenic processes that led to the amalgamation of the Western Gondwana supercontinent (Heilbron et al., 2017; Teixeira et al., 2017). The Archean blocks of the SFC record a long geological history broadly including Meso- to Neoarchean (ca. 3.0 – 2.7 Ga) episodes of continental crust formation and collision of continental fragments at ca. 2.7–2.6 Ga (Machado et al., 1996b; Noce et al., 1998; Campos et al., 2003; Lana et al., 2013; Albert et al., 2016). This was followed in the Archean-Paleoproterozoic transition by rifting and accumulation of passive margin successions such as the Minas Supergroup (Nutman and Cordani, 1993; Martin et al., 1997; Barbosa et al., 2013; Dantas et al., 2013; Farina et al., 2016; Teixeira et al., 2017).

This contribution reports new lithogeochemical, whole-rock Nd and zircon U-Pb-Hf isotopic data from Archean granite-greenstone belt associations located in the southernmost portion of the SFC, known as the Campos Gerais Complex (CGC). The new data, integrated with geochemical and isotopic data published by Turbay and Valeriano (2012), reveal an important subduction-collision cycle marking the first Archean TTG-sanukitoid association within the southernmost SFC. This study also presents a comparison of the tectonic evolution of the CGC with that of the other Archean complexes of the southern SFC, and a discussion of tectonic scenarios for the Archean evolution.

2. Archean blocks in the São Francisco craton

Several Archean blocks have been identified both in the northern and southern portions of the SFC where the (pre-1.8 Ga) basement complexes are exposed (Fig. 1). In the northern SFC, the Archean blocks were amalgamated during the Rhyacian-Siderian, forming the Eastern -Bahia orogen (Barbosa and Barbosa, 2017 and references therein). From west to east (Fig. 1) they are the Gavião-Cristalândia do Piauí, Guanambi-Correntina, Sobradinho, Jequié, Salvador-Itabuna-Curaçá, and Serrinha blocks. The Gavião-Cristalândia do Piauí and Guanambi-Correntina blocks contain the oldest record of TTG magmatism in the SFC, with ages between ca. 3.65–3.26 Ga and between ca. 3.18–3.00 Ga, respectively (Nutman and Cordani, 1993; Cruz et al., 2012; Dantas et al., 2013; Teixeira et al., 2017; Barbosa et al., 2020; Oliveira et al., 2020). Greenstone-belt type supracrustal associations are described in the Gavião and other blocks with ages between 3.40 Ga and 3.26 Ga, as well as in the ca. 2.75– 2.50 Ga interval (Bastos-Leal et al., 2003; Peucat et al., 2003; Oliveira et al., 2010; Paquette et al., 2015; Teixeira et al., 2017). Neoarchean TTG associations are widespread in all tectonic blocks (Oliveira et al., 2010; Barbosa et al., 2013; Silva et al., 2016). Layered mafic–ultramafic intrusions of ca. 2.58 Ga have also been described in the Eastern Bahia orogen, in northeastern SFC (Oliveira et al., 2010; Piaia et al., 2017).

The southern portion of the SFC (Fig. 2) comprises several Archean granite-gneiss complexes (Campo Belo, Divinópolis, Bonfim, Passa Quatro, Belo Horizonte, Santa Barbara, Guanhães and Bação), supracrustal associations (Rio das Velhas and Pitangui greenstone belts) and mafic–ultramafic layered intrusions. Paleoproterozoic units are represented by the supracrustal associations (Minas Supergroup), isolated granitic intrusions (e. g. Porto Mendes granite) and, to the south, accreted terranes such as the Mineiro belt (Alkmim and Teixeira, 2017) and the Mantiqueira Complex during the Rhyacian-Siderian (Bruno et al., 2020).

The Archean granite-gneiss-migmatite complexes consist predominantly of TTG magmatic associations with ages ranging from ca. 2.9 Ga to 2.65 Ga (Teixeira et al., 1996; Noce et al., 1998; Lana et al., 2013; Farina et al., 2015). TTG rocks older than 2.9 Ga have until now been described only in the Campo Belo (ca. 3.2–3.05 Ga; Teixeira et al., 1996) and Santa Bárbara (ca. 3.2 Ga; Lana et al., 2013) complexes. The presence of older continental crust is indicated by Paleoarchean detrital zircon in younger metasedimentary sequences, as evidenced by inherited fractions of igneous zircons (Machado et al., 1996b; Hartmann et al., 2006; Lana et al., 2013; Moreira et al., 2016) and T_{DM} Nd model ages of TTG associations (De Paolo, 1981; Carneiro et al., 1998; Teixeira et al., 2017).

The Pitangui, Rio das Velhas and Fortaleza de Minas are the main greenstone-belt associations in the southern SFC (Fig. 2), with depositional ages constrained at ca. 2.86 Ga respectively by detrital zircon (Soares et al., 2020) and Sm–Nd isochron (Pimentel and Ferreira Filho, 2002). The Rio das Velhas greenstone belt has a minimum depositional age of 2.88 Ga, constrained by detrital zircons (Machado et al., 1996b; Moreira et al., 2016), and evolved at least until 2.75 Ga, which is the age of the youngest felsic volcanic rocks (Machado et al., 1992; Noce et al., 2005).

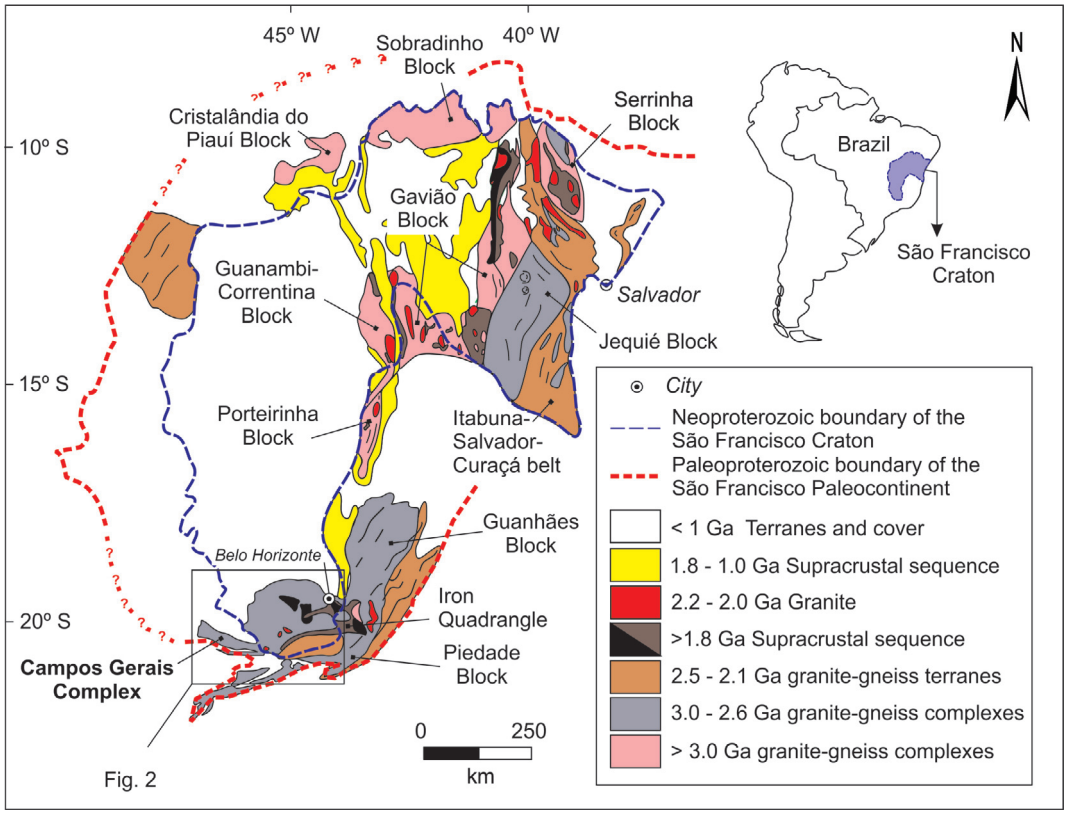

Fig. 1. Main pre-1.0 Ga tectonic units of the São Francisco Craton (blue dashed line) and the extended older paleocontinental limit (red dashed line). Major Archean and Paleoproterozoic complexes are highlighted. Modified after Bruno et al. (2020), Bersan et al. (2018), Zincone et al. (2020), Degler et al. (2018), Alkmim and Teixeira (2017), and Barbosa and Barbosa (2017).

In the southernmost portion of the SFC, a granite-greenstone lithological association, generally referred to as the Campos Gerais complex, the focus of this study, is exposed in a tectonic window between overlying nappe complexes related to the Neoproterozoic Brasilia orogenic belt. A review of the geology of the Campos Gerais complex recently presented by Pinheiro et al. (in press), describes predominant TTG and other granitoid/orthogneises and migmatites, with supracrustal lenses, some of which have greenstone-belt characteristics. The Campos Gerais complex underwent amphibolite to granulite facies metamorphism with variable degrees of retrogression to greenschist facies conditions.

Granite-greenstone associations also occur in the *para*-autochthonous foreland thrust-fold belt of the surrounding Neoproterozoic orogenic belts and likely represent reworked segments of the basement of the SFC continental margin. In the external Southern Brasilia orogen, the Piumhi granite-greenstone sliver (Fig. 2) displays a volcano-sedimentary succession older than 3.1 Ga (Machado and Schrank, 1983), which includes basal komatiitic basalts with pillow structures, intruded by TTG tonalites and granodiorites with a TIMS U–Pb zircon age of 2935 ± 3 Ma (Valeriano et al., 2004).

3. Analytical procedures

The detailed analytical procedures for each technique used here are given in Supplementary Data A. Sample preparation was performed in the Laboratório Geológico de Processamento de Amostras lab at UERJ (Brazil). U–Pb geochronological data was obtained on zircon separates using LA-MC-ICPMS techniques at the University of Alberta (Canada) and LA-ICPMS at the University of Portsmouth (UK). The Lu–Hf isotopic determinations were conducted in the latter university using LA-MC-ICPMS. Whole rock Sm–Nd analyses were performed using standard ID-TIMS techniques at the Laboratório de Geocronologia e Isótopos Radiogênicos -LAGIR laboratory at UERJ (Brazil). Whole rock major and trace element chemical analyses were performed by Activation Laboratories Inc. (Ancaster, Canada).

4. Results

The new results reported here are: field observations carried out in the two study areas, which resulted in a new geological map for the area south of Alpinópolis town (Fig. 3); LA-ICPMS U–Pb analyses for five samples from the Alpinópolis area and two from the Minduri area (Fig. 4, samples MA-JF-48C and MA-JF-49B); whole-rock major and trace element compositions, Sm–Nd isotope compositions for the two Minduri samples; and Hf isotopic compositions of zircons from sample MA-JF-49B.

The new data are presented and discussed in integration with the previously published data from the study area in the south of Alpinópolis, including geochemical compositions from 27 samples and Sm–Nd isotopic results from six of those samples (Turbay and Valeriano, 2012); the latter are the focus on six of the new U–Pb analyses reported here. The coordinates, geochemical classification and analytical data available for each studied sample are displayed in Supplementary Data B.

4.1. Field geology features of the south of Alpinópolis town

The area south of Alpinópolis town (Fig. 3) can be generally referred to as a granite-greenstone terrain with a variety of more or less deformed granitoid rocks and isolated greenstone keels

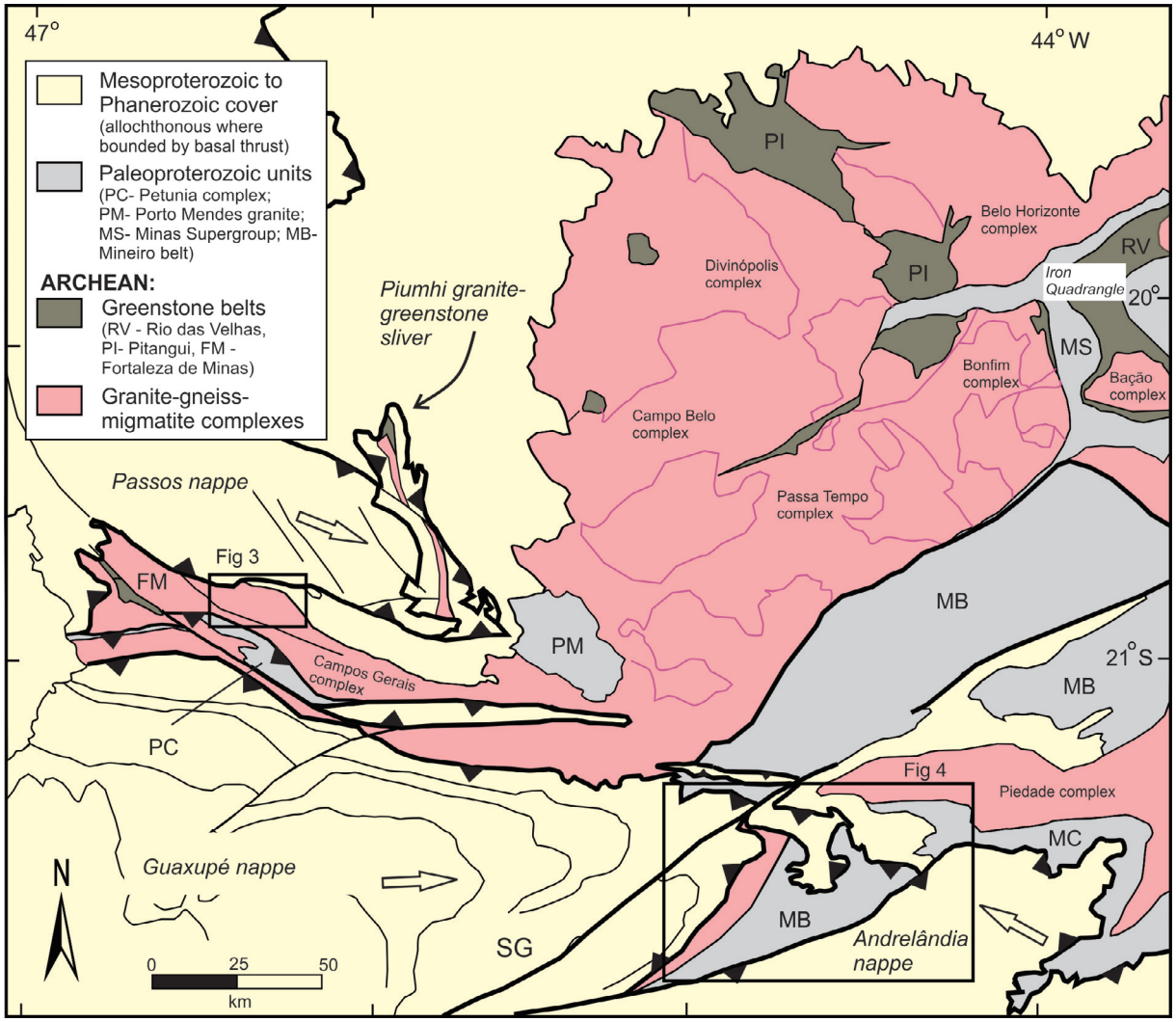

Fig. 2. Tectonic units of the southern São Francisco craton (modified after Pinto and Silva, 2014), with location of Figs. 3 and 4 study areas. FM – Fortaleza de Minas Greenstone Belt; PC – Petúnia Complex; PM – Porto dos Mendes Granite; SG – Socorro-Guaxupe Nappe; PI – Pitangui Greenstone Belt; RV – Rio das Velhas Greenstone Belt; MS – Minas Supergroup; MB – Mineiro Belt; MC – Mantiqueira Complex.

intruded by elliptical plutonic bodies. A general deformation gradient is observed, where strain is low or absent in the northeastern portion, becoming higher to the southeast. To the northeast, the CGC orthogneisses display a weak foliation dipping moderately to the SE, which however does not completely obliterate the primary igneous features. To the southeast, the orthogneisses become progressively more deformed, where an anastomosed network of sinistral NW-trending mylonite to ultramylonite zones defines lens-shaped orthogneiss domains. The latter display a pervasive foliation, commonly protomylonitic, and affected by open to tight folds. Discrete brittle shear zones generate localized cataclasites in both domains.

Four main lithological associations are recognized in the field and were mapped (Fig. 3), taking into account petrographic and geochemical data from Turbay et al. (2008) and Turbay and Valeriano (2012): (a) in the central portion of the study area grey banded biotite (±hornblende) tonalites and granodiorites (of TTG affinity, see geochemical section below) predominate. They commonly contain amphibolite layers and lenses and display ubiquitous migmatization features, such as leucosome veins surrounded by biotite-hornblende-rich melanosomes, locally evolving to diatexite, and cross-cut by leucogranite veins and larger bodies of outcrop and map scale (Fig. 5a, b); (b) greenstone-belt type supracrustal associations occur in the northern part of the area, outcropping as deeply weathered patches of chlorite-tremolite schists and serpentinites; (c) biotite (±muscovite) leucogranites and gneissic varieties (Fig. 5c) predominate in the northern and southern portions of the area (Fig. 3), either in homogeneous exposures or with diatexitic structure. Biotite-rich lenticular (schlieren) residue is frequent, and consistent with the geochemical signature of hybrid and peraluminous crust-derived granites (as discussed below); and (d) several intrusive elliptical stocks of homogeneous, essentially undeformed tonalite occur in the northern and central portions of the area (Fig. 3). They commonly display subvolcanic textures with plagioclase phenocrysts embedded in a fine-grained matrix (Fig. 5d, e), which are suggestive of shallow levels of emplacement. Mafic clots that contain biotite and hornblende are also common.

All lithologic units display retrogressive mineral associations, such as saussurite and sericite in feldspar, epidote in intermediate to felsic rocks and chlorite associated with biotite and hornblende.

4.2. Field geology of the area around Minduri town

The second studied area (Fig. 4) is located among the east-verging thrust sheets of the Southern Brasília belt (Campos Neto,

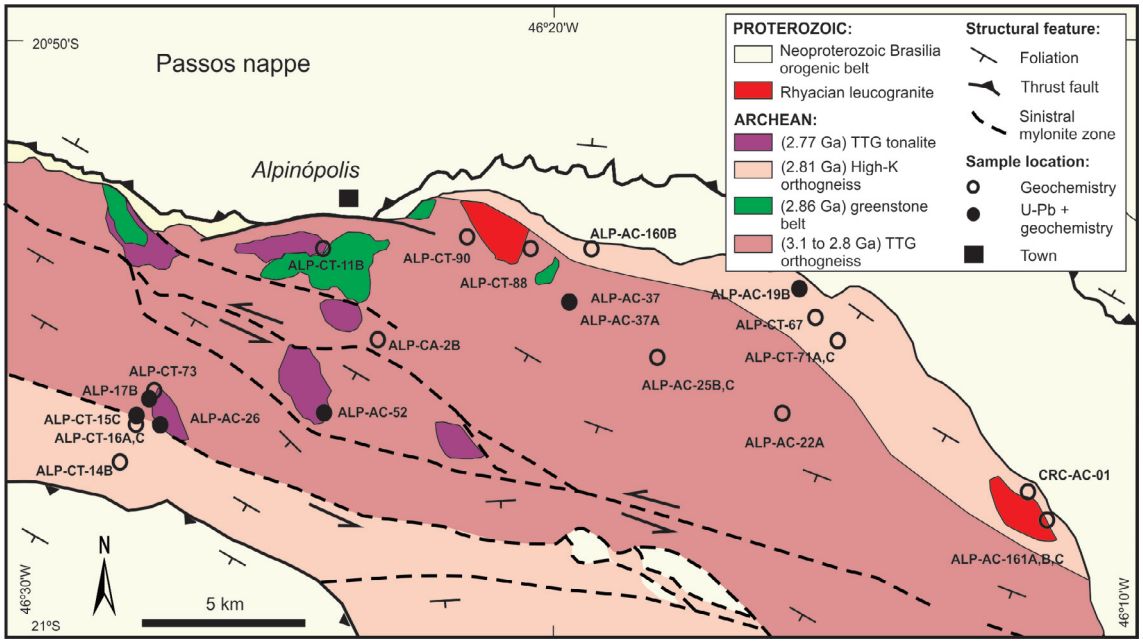

Fig. 3. Geological simplified map of the area south of Alpinópolis town, with the location of studied samples. Geochemical data from Turbay and Valeriano (2012).

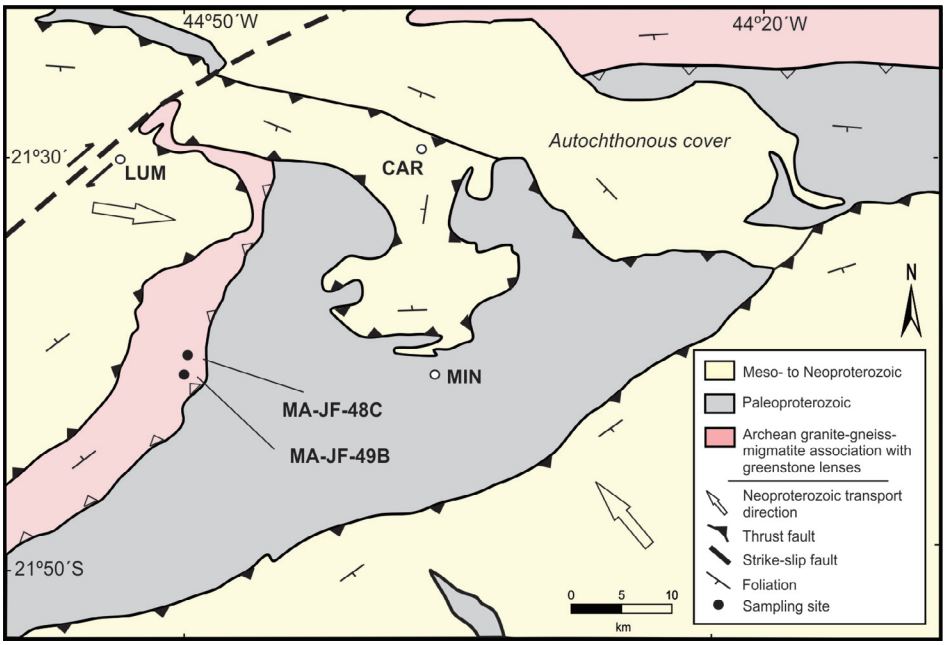

Fig. 4. Geological sketch map of the Minduri town (MIN) area, with the location of studied samples in the Archean inlier among Neoproterozoic rocks. LUM – Luminárias, MIN - Minduri, CAR – Carrancas towns.

2000; Trouw et al., 2002, 2013; Valeriano et al., 2004), partly overprinted by the tectono-metamorphic events of the younger Ribeira belt (Machado et al., 1996a) (Fig. 4). Basement associations occur in one large sliver between two Neoproterozoic metasedimentary thrust sheets (Andrelândia Group). Bruno et al. (2021) and Trouw et al. (2002) divided the basement associations into two different thrust sheets that occur among other ones of Neoproterozoic metasedimentary rocks and underwent Neoproterozoic regional lower amphibolite facies metamorphism and deformation. The upper and western thrust sheet (Fig. 4), which was sampled for geochemical and isotopic (U–Pb, Lu–Hf, Sm–Nd) investigation, comprises a granite-greenstone lithological association. Coarse-grained mesocratic orthogneisses predominate, frequently cross cut by leucosome veins. Lenses of *meta*-ultramafic rocks and amphibolite (Fig. 5f) are common within the orthogneisses. The lower basement thrust sheet (Fig. 4) is represented predominantly by Paleoproterozoic biotite-hornblende orthogneisses studied by Cioffi et al. (2016) and Bruno et al. (2021).

A coarse-grained tonalite sampled for study (sample MA-JF-49B) was characterized as a sanukitoid and selected for U–Pb, Sm–Nd and Lu–Hf analyses. Detailed petrographic description is given in Supplementary Data C.

Fig. 5. Representative lithologic varieties of the Campos Gerais complex: (a) TTG tonalite and high-K leucogneiss. Hammer = 50 cm (ALP-AC-90); (b) TTG 2971 ± 31 Ma tonalite. Hammer = 50 cm (ALP-AC-37A); (c) foliated 2820 ± 69 Ma peraluminous biotite granite (ALP-AC-19B); (d) late intrusive 2792 ± 29 Ma TTG tonalite (ALP-AC-52); (e) Sanukitoid 2891 ± 19 Ma orthogneiss west of Minduri town (MA-JF-49B), injected by leucogranite (GPS cap for scale = 25 cm); (f) tholeiitic 2669 ± 24 Ma amphibolite (MA-JF-48C) west of Minduri town.

4.3. Whole rock element composition

The new geochemical data from two samples reported here are combined with previous data published by Turbay and Valeriano (2012), totaling 28 samples. The major and trace element compositions are given in Supplementary Data D.

Based on field and geochemical data, the granitoid rocks, amphibolite and orthogneisses of the CGC were classified using commonly adopted discriminant diagrams based on major and trace element compositions in widely used discriminant diagrams shown in Figs. 6 and 7. Additionally, they were further separated into compositional groups according to the classification of Archean granitoid rocks from Laurent et al. (2014). In the ternary diagram of Fig. 7b, they are separated into TTG, sanukitoid, hybrid and biotite/two-mica granitoids. In Fig. 7c, the discriminant diagram displays fields for possible source rocks based on an extensive petrogenetic data base.

The studied samples were thus geochemically classified into the following compositional groups: (1) TTG orthogneisses; (2) high-K hybrid granites; (3) high-K peraluminous granites; (4) intrusive TTG tonalites; (5) one sample with a typical sanukitoid signature; and (6) one tholeiitic metabasic rock.

4.3.1. TTG orthogneisses

The TTG orthogneisses plot within the granodiorite and granite fields in the SiO_2 vs. $Na_2O + K_2O$ diagram (Fig. 6a) and in the trondhjemite field on the basis of the normative feldspar classification diagram for granitoids (Fig. 6b). They are silica-rich (64–75 wt.%) and have high Na_2O/K_2O ratios (2.1–4.9), relatively poor abundances in ferromagnesian elements and high concentrations of incompatible elements such as Ba, Sr, low Y. They are also characterized by moderate Sr/Y ratios (8 – 58) and low concentrations of compatible trace elements (V, Ni, Cr). The samples also display moderate contents of high-field-strength-elements (HFSE) such as Nb and Zr. They plot within the medium-K calc-alkaline series field of the SiO_2 vs. K_2O diagram (Fig. 6c), within the magnesian field of the $FeO_t/(FeO_t + MgO)$ diagram (Fig. 6d), and are classified as metaluminous to slightly peraluminous using the A/NK vs. A/CNK discrimination diagram (Fig. 7a).

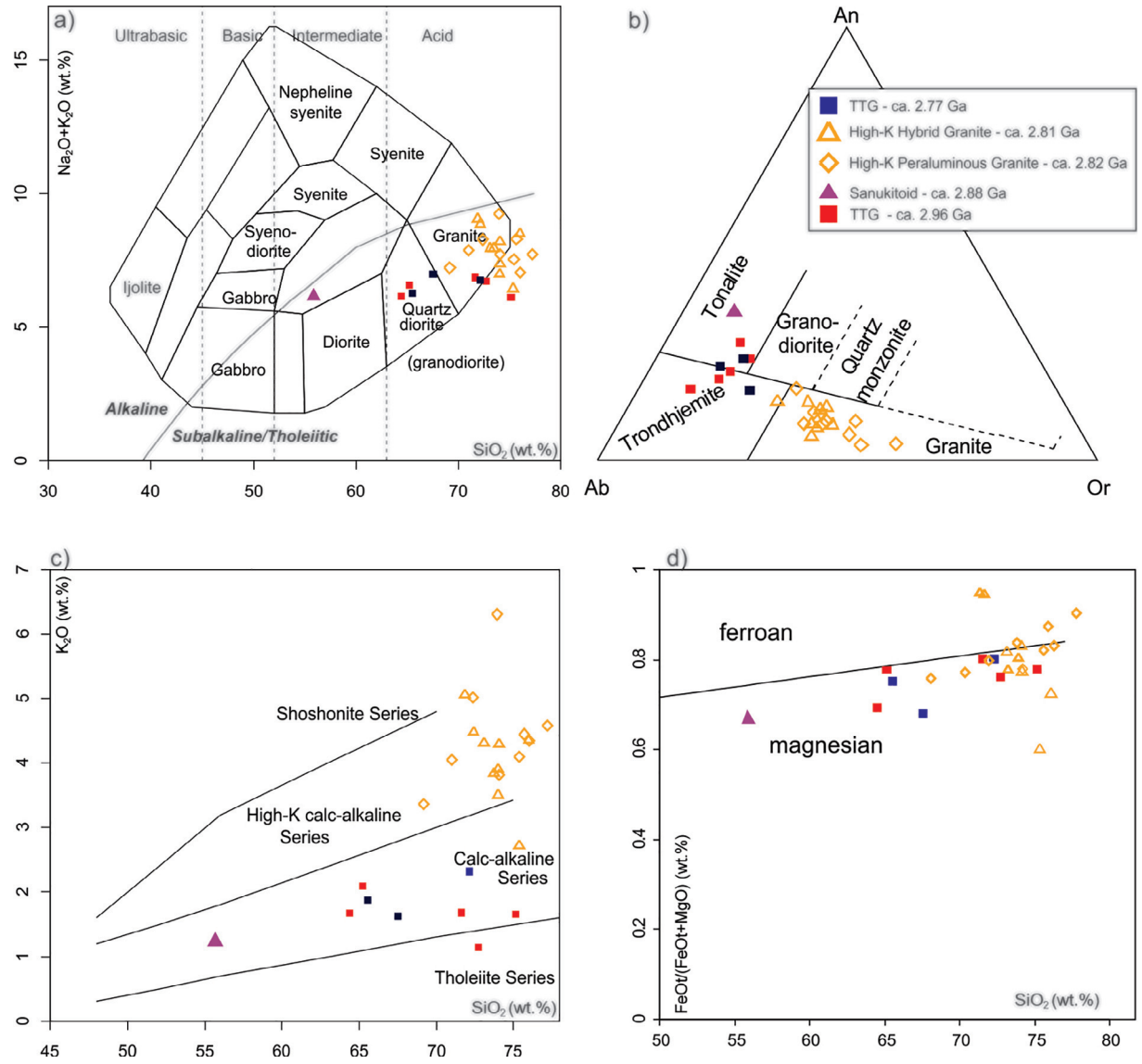

Fig. 6. Major element composition characteristics of the studied samples (ages from this work). (a) SiO_2 vs. $Na_2O + K_2O$ classification diagram (Cox et al., 1979); (b) Classification diagram for siliceous igneous rocks, based on normative feldspar composition (O'Connor, 1965); (c) SiO_2 vs. K_2O diagram (Peccerillo and Taylor, 1976); (d) FeO_t / (FeO_t + MgO) vs. SiO_2 diagram (Frost et al., 2001).

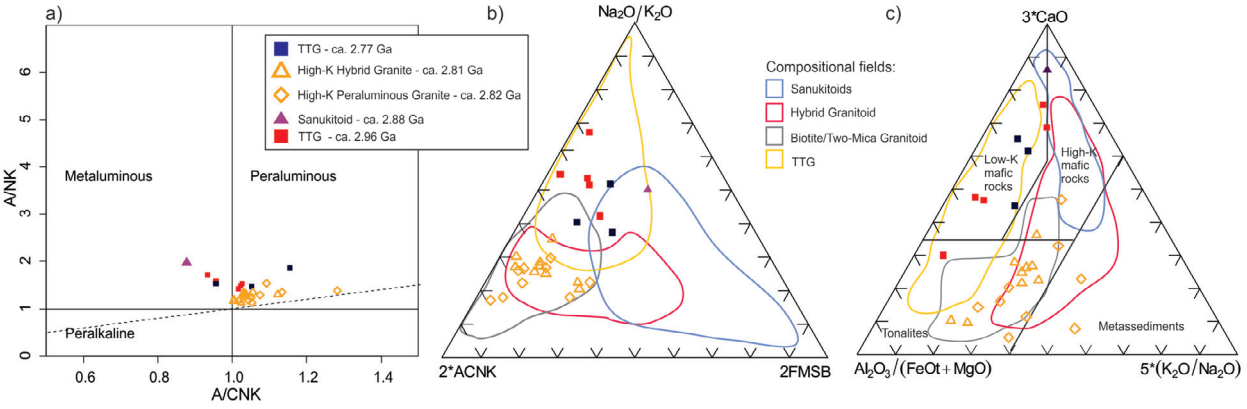

Fig. 7. Discriminant diagrams for the studied samples (ages from this work). (a) A/NK vs. A/CNK diagram (Shand, 1943); (b) Classification diagram of Laurent et al. (2014). Vertices are: 2 × (molar Al_2O_3 / ($CaO + K_2O + Na_2O$); Na_2O/K_2O and 2 × (FeO_t + MgO) × (Sr + Ba); (c) Ternary Al_2O_3 / (FeO_t + MgO); 3 × CaO; 5 × (K_2O/Na_2O) diagram showing potential source of melts (Laurent et al., 2014).

In the petrogenetic indicator diagrams of Laurent et al. (2014) (Fig. 7b, c) they are strictly TTG rocks with dominantly low-K mafic rocks as their source. In the chondrite-normalized REE diagram (Fig. 8a), samples show enrichment of the light rare earth elements (LREEs) compared to the heavy rare earth elements (HREEs). They have high $(La/Yb)_N$ ratios ($12 < (La/Yb)_N < 31$) and lack significant

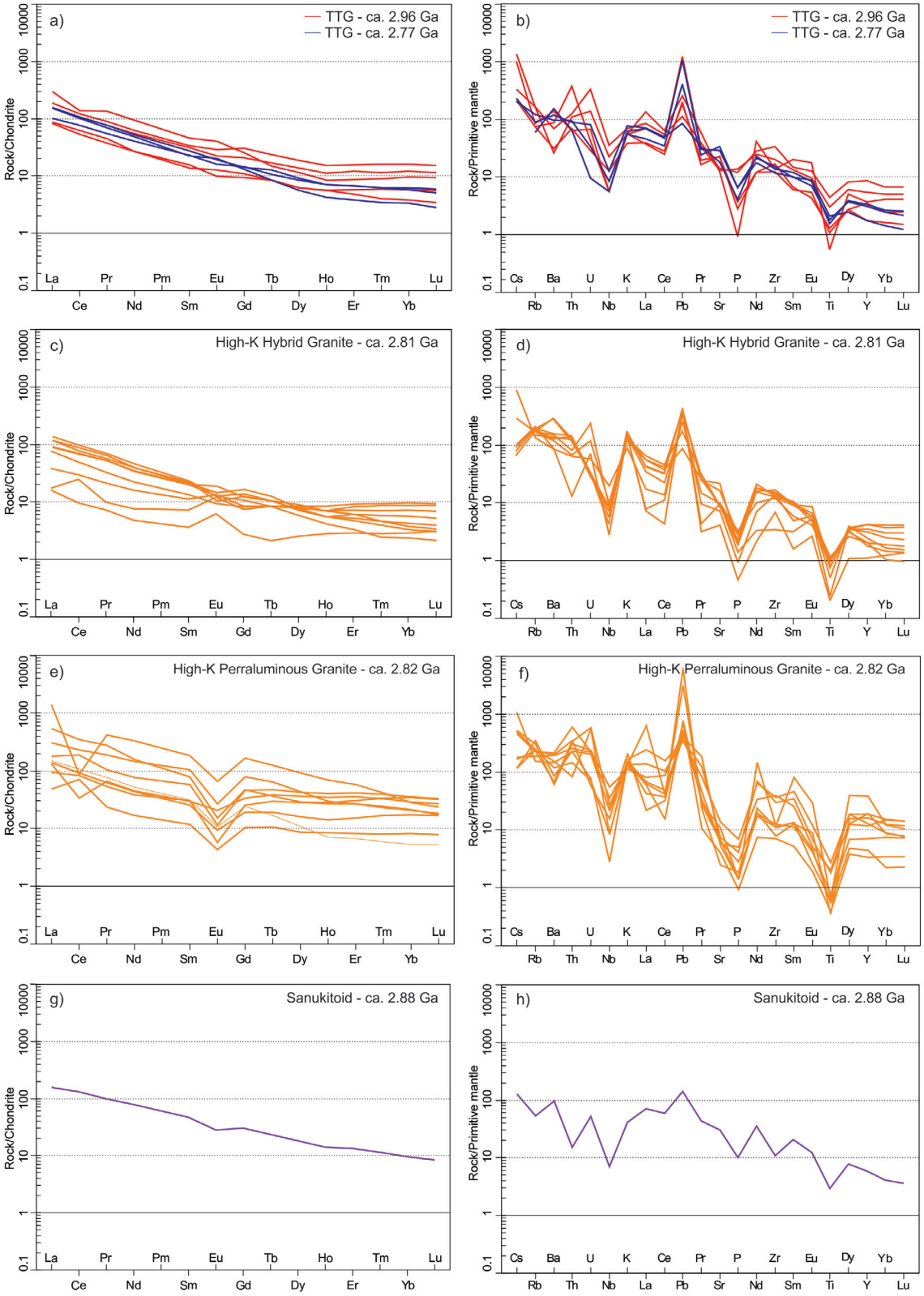

Fig. 8. Left column: chondrite-normalized REE diagrams (Boynton, 1984). Right column: primitive mantle-normalized multielement plots (McDonough and Sun, 1995). (a, b) TTG orthogneiss; (c, d) High-K hybrid granite; (e, f) High-K peraluminous granite; (g, h) Sanukitoid tonalite.

Eu anomalies (0.8 < Eu/Eu* < 1.2). In the primitive mantle normalized diagram (Fig. 8b), the samples exhibit positive Pb anomalies and negative Nb, P and Ti anomalies.

4.3.2. High-K hybrid granites

The high-K hybrid granites plot in the granite fields of the SiO_2 vs. $Na_2O + K_2O$ and of the normative feldspar classification diagram for granitoid rocks (Fig. 6a, b). The samples display high SiO_2 contents (71.9 wt.%<SiO_2 < 76 wt.%), low Na_2O/K_2O ratios (0.8 – 1.4), Al_2O_3 between 13.1 wt.% and 15 wt.% and Cr and Ni below < 20 ppm. They plot within the high-K calc-alkaline series field of the SiO_2 vs. K_2O diagram (Fig. 6c), and along the boundary between magnesian and ferroan fields of the $FeO_t/(FeO_t + MgO)$ diagram (Fig. 6d). Their major elements also define them as having *meta*-aluminous to slightly peraluminous compositions (Fig. 7a).

According to Laurent et al. (2014), the high-K hybrid granites (Fig. 7b) are the product of melting of tonalites (Fig. 7c). In the REE chondrite-normalized diagram (Fig. 8c), this compositional group shows little to high LREE enrichment relative to HREE ($1.99 < La/Yb_N < 59.19$), and variable Eu anomalies ($0.63 < Eu/Eu^* < 1.97$). In mantle-normalized trace element diagrams (Fig. 8d), they are characterized by enrichment of LILE (large-ion lithophile elements), depletion in Nb, P and Ti abundances, and positive Pb and K anomalies.

4.3.3. High-K peraluminous granites

Samples classified here as peraluminous high-K granites are characterized by high silica contents (SiO_2 > 69 wt.%), low concentrations of ferromagnesian oxides ($FeO_t + MgO + MnO + TiO_2$ < 5 wt.%), CaO (<2 wt.%), low Na_2O/K_2O ratios (<1), and moderate Al_2O_3 leading to high $Al_2O_3/(FeO_t + MgO)$ ratios. Samples plot within the granodiorite and granite fields of the SiO_2 vs. $Na_2O + K_2O$ diagram, the high-K calc-alkaline series field of the SiO_2 vs. K_2O diagram, at the boundary between the magnesian and ferroan fields of the $FeO_t/(FeO_t + MgO)$ diagram, and are classified as peraluminous (Fig. 6a, b, c, d). This compositional group plots within the granite field of the normative feldspar classification diagram for granitoids. In the petrogenetic indicator ternary diagram, they plot in the biotite/two-mica granitoid field, which characterize them as melt products of tonalites and metasedimentary rocks (Fig. 7a, b, c).

These samples have low HFSE and transition element contents such as Zr and V, and Ba/Rb and Sr/Y ratios. REE chondrite-normalized diagrams show moderate fractionation of REE patterns ($7 < La/Yb_N < 49$) but significant negative Eu anomalies between 0.21 and 0.80 (Fig. 8g). The primitive mantle normalized diagram (Fig. 8h) shows high contents of highly incompatible elements such as Rb and Th and enrichment in Ba abundances.

4.3.4. Sanukitoid hornblende gneiss (sample MA-JF-49B)

The coarse-grained mesocratic hornblende-bearing orthogneiss sample MA-JF-49B (Fig. 5) is a normative tonalite of calc-alkaline affinity, plotting in the intermediate (diorite) field of the TAS diagram (Fig. 6a), and in the medium-K field of the SiO_2 vs. K_2O diagram (Fig. 6c). It is characterized by high CaO and ferromagnesian oxides ($FeO_t + MgO + MnO + TiO_2$ = 11 wt.%), with magnesian and metaluminous ($0.7 \leq A/CNK \leq 1.0$) character (Fig. 6d and 7a).

In the petrogenetic indicator ternary diagram of Laurent et al. (2014) the sample plots in the overlap zone between the TTG and sanukitoid fields (Fig. 7b). However, according to the well-established criteria of Laurent et al. (2014), Heilimo et al. (2010) and Martin et al. (2009), this sample has distinguishing compositional features that classify it as a sanukitoid, such as relatively high concentrations of compatible trace elements (Ni = 50 ppm, Cr = 40 ppm, V = 108 ppm) and of LILE (K_2O = 1.23 wt.%, Ba = 675 ppm, Sr = 639 ppm). Other compositional features preclude a TTG classification, such as the low SiO_2 content (56 wt.%), high Y (27 ppm) and low La_N/Yb_N relative to Yb_N (Martin, 1986). As an additional distinguishing feature from TTG rocks, the sample plots within the sanukitoid field in the major element diagram of Laurent et al. (2014) in Fig. 7c.

The chondrite normalized REE patterns show enrichment in LREE relative to HREE and small negative Eu anomalies (Fig. 8g). In the primitive mantle normalized diagram, the sample shows enrichment in fluid mobile LILEs (Ba, Rb and K) and Pb (Fig. 8h).

4.3.5. Intrusive TTG tonalites

Three tonalite samples (ALP-AC-11B, ALP-AC-26, ALP-AC-52) were collected from relatively undeformed elliptical intrusive bodies (Fig. 3). They have similar major element features as the TTG orthogneisses described above (Figs. 6 and 7), but a more aluminous composition and more differentiated chondrite-normalized REE pattern (Fig. 8 a, b).

4.3.6. Tholeiitic metabasic rocks

Amphibolites from the Minduri area, which occur as enclaves within the intermediate to felsic orthogneisses, are represented by sample MA-JF-48C, which has a gabbroic composition in the tholeiitic series (Fig. 6a), characterized by low-TiO_2 (<2 wt.%), low Mg# and high contents of both CaO and Al_2O_3.

The chondrite-normalized REE plot shows a flat pattern ($La_N/Yb_N \leq 3$) and small negative to absent Eu anomalies ($0.97 \leq Eu_N/Eu^* \leq 1$) consistent with the signature of a normal-type mid-ocean ridge basalt (N-MORB). In the N-MORB-normalized multi-element diagram, the sample shows relative enrichment of incompatible elements such as K, Ba, La and Rb, and depletion of Ti, Nb and Sr.

4.4. Zircon U–Pb geochronology

Six samples from the CGC south of Alpinópolis town (Fig. 3) and two from the Minduri area (Fig. 4) were selected. Analytical results are given in Supplementary Data E.

The age results for the studied samples are presented below in chronological order based on their interpreted crystallization ages. It is important to notice that, as discussed further below, probably due to the polycyclic tectonic evolution of the studied area, almost all of the analyzed zircon grains are variably discordant. Nevertheless, they define discordia lines with lower intercepts reflecting lead loss related to well-known Paleoproterozoic or Neoproterozoic metamorphic events, such as in the Rhyacian (Alkmim and Teixeira, 2017) or related to the Brasiliano event (Heilbron et al., 2017), respectively. Therefore, the discordia lines presented below, although displaying relatively poor regression (high MSWD), yield upper intercept ages that are regarded as geologically meaningful, even taking into account their age errors.

4.4.1. High-K hybrid granite (sample ALP-AC-17B)

Sample ALP-AC-17B is a foliated granitic orthogneiss belonging to the high-K hybrid granite compositional group (Fig. 3). This sample has predominantly short prismatic pink zircon grains, some with overgrowth rims (Fig. 9a). Seventeen zircon grains were analyzed, all with discordance between 7% and 21%. The distribution of data points in the Wetherill diagram does not allow a statistically meaningful crystallization age for the rock to be constrained (Fig. 9a). However, the data define two clusters, two older individual grains and one younger metamorphic overgrowth which provide some useful geological information. An isolated data point (#13) has a $^{207}Pb/^{206}Pb$ age of 2912 ± 16 Ma (19.3% discordant), which is regarded as a minimum age of crystallization (see Sm–Nd data below). A cluster of five grains has a weighted average

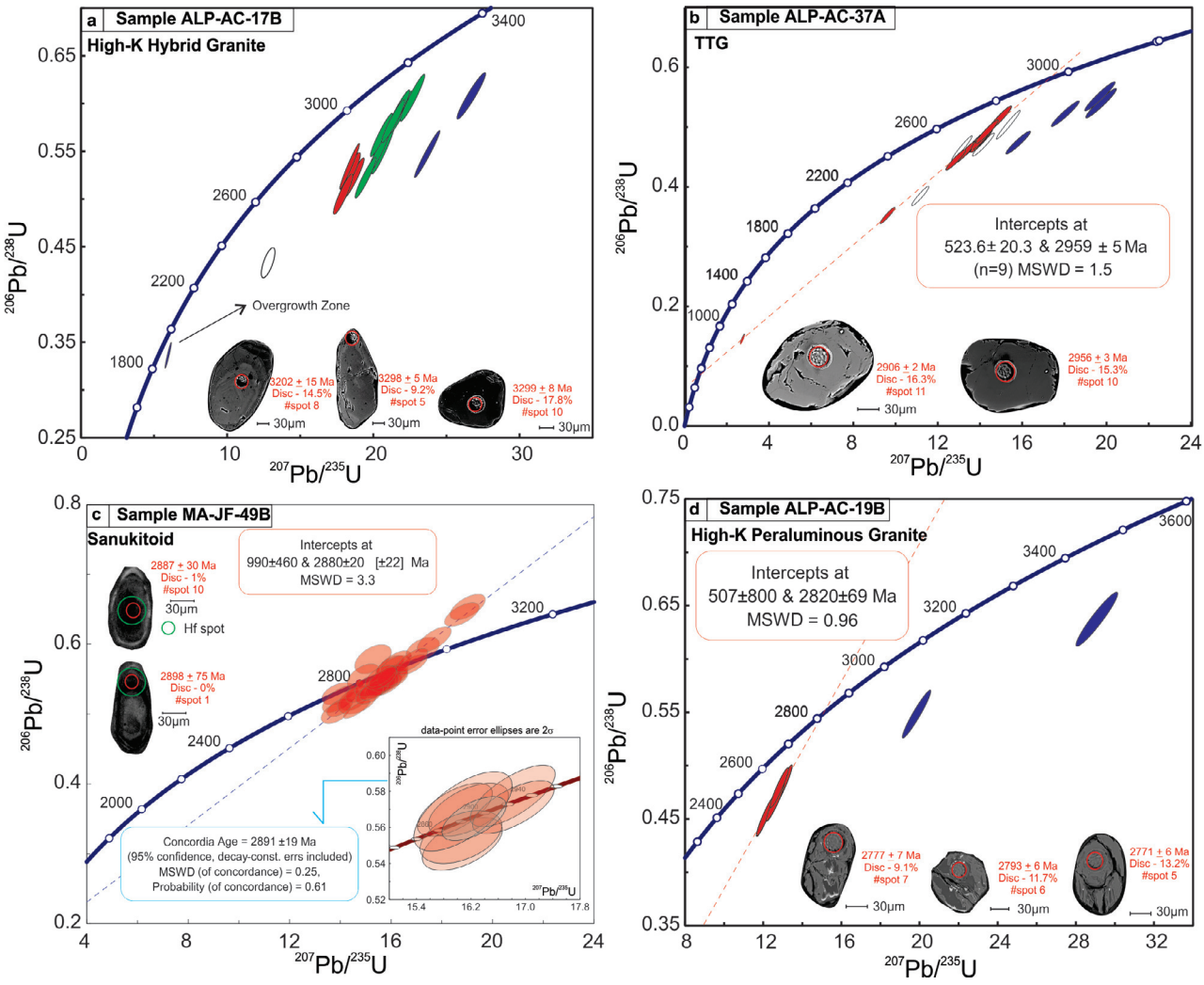

Fig. 9. LA-ICPMS U–Pb concordia diagrams of the Archean granitoid rocks of the Campos Gerais Complex. (a) High-K hybrid granite II (sample ALP-AC-17B); (b) High-K hybrid granite I (sample ALP-AC-37A); (c) Sanukitoid tonalite (sample MA-JF-49B); (d) High-K peraluminous granite (sample ALP-AC-19B).

of $^{207}Pb/^{206}Pb$ dates of ca. 3.19 Ga (MSWD = 0.05, probability = 0.995), and an older cluster of nine grains has a weighted average of $^{207}Pb/^{206}Pb$ dates of 3.29 Ga (MSWD = 0.09, probability = 1.000). Two additional inherited grains with $^{207}Pb/^{206}Pb$ ages of 3540 ± 3 Ma (21% disc.) and of 3562 ± 3 Ma (14% disc.). One measurement spot (#6) from a zone of new growth around the core zone (Corfu et al., 2003), yielded a $^{207}Pb/^{206}Pb$ age of 2075 ± 4 Ma (9.9% discordant).

4.4.2. TTG trondhjemitic orthogneiss (sample ALP-AC-37A)

Sample ALP-AC-37A is a homogeneous, medium-grained mesocratic trondhjemitic orthogneiss belonging to the TTG compositional group (Figs. 3 and 5a). Twenty-one zircon grains were analyzed, and these are typically translucent, pink euhedral short prisms (2:1 to 3:1 aspect ratios). Four grains (blue ellipses in Fig. 9b) yield relatively older dates, with $^{207}Pb/^{206}Pb$ ages of 3129 ± 5 Ma, 3182 ± 2 Ma, 3230 ± 10 Ma and 3273 ± 11 Ma. Nine of the younger grains define a discordia line with an upper intercept age of 2959 ± 5 Ma and a lower intercept age of 524 ± 20 Ma (MSWD = 1.6).

4.4.3. Sanukitoid tonalite (sample MA-JF-49B)

Sample MA-JF-49B is from the hornblende tonalitic gneiss of sanukitoid composition from the Minduri inlier (Figs. 4 and 5e). Zircons are typically prismatic, translucent and of yellowish color showing fine igneous oscillatory zoning. Twenty-four analyses of concordant to sub-concordant grains yield a discordia line with an upper intercept of 2880 ± 20 Ma and lower intercept of 990 ± 460 Ma (MSWD = 3.3) (Fig. 9c). The seven most concordant zircon grains yield a concordia age of 2891 ± 19 Ma (MSWD = 0.25), interpreted as the crystallization age of the rock.

4.4.4. High-K peraluminous granites

Sample ALP-AC-19B is a foliated high-K peraluminous biotite leucogranite belonging to the biotite/two mica granite compositional group (Fig. 3). Seven grains were analyzed, from which five euhedral, short, prismatic grains define a discordia line yielding an upper intercept of 2820 ± 69 Ma (MSWD = 0.96) (Fig. 9d), interpreted as the crystallization age. Two other discordant grains yield older $^{207}Pb/^{206}Pb$ ages of 3621 ± 4 Ma and of 3620 ± 6 Ma.

Sample ALP-AC-15 is a coarse-grained peraluminous leucogranite (Fig. 3). Zircon grains are euhedral, brownish, short prisms from which 10 were analyzed. Seven zircon grains define a discordia line yielding an upper intercept age of 2812 ± 15 Ma (MSWD = 0.81) (Fig. 10a), interpreted as the crystallization age, and a lower intercept age of 570 ± 26 Ma. Two discordant analyses (spots # 1 and #8) yield older $^{207}Pb/^{206}Pb$ ages of 3084 ± 13 Ma and 3412 ± 5 Ma.

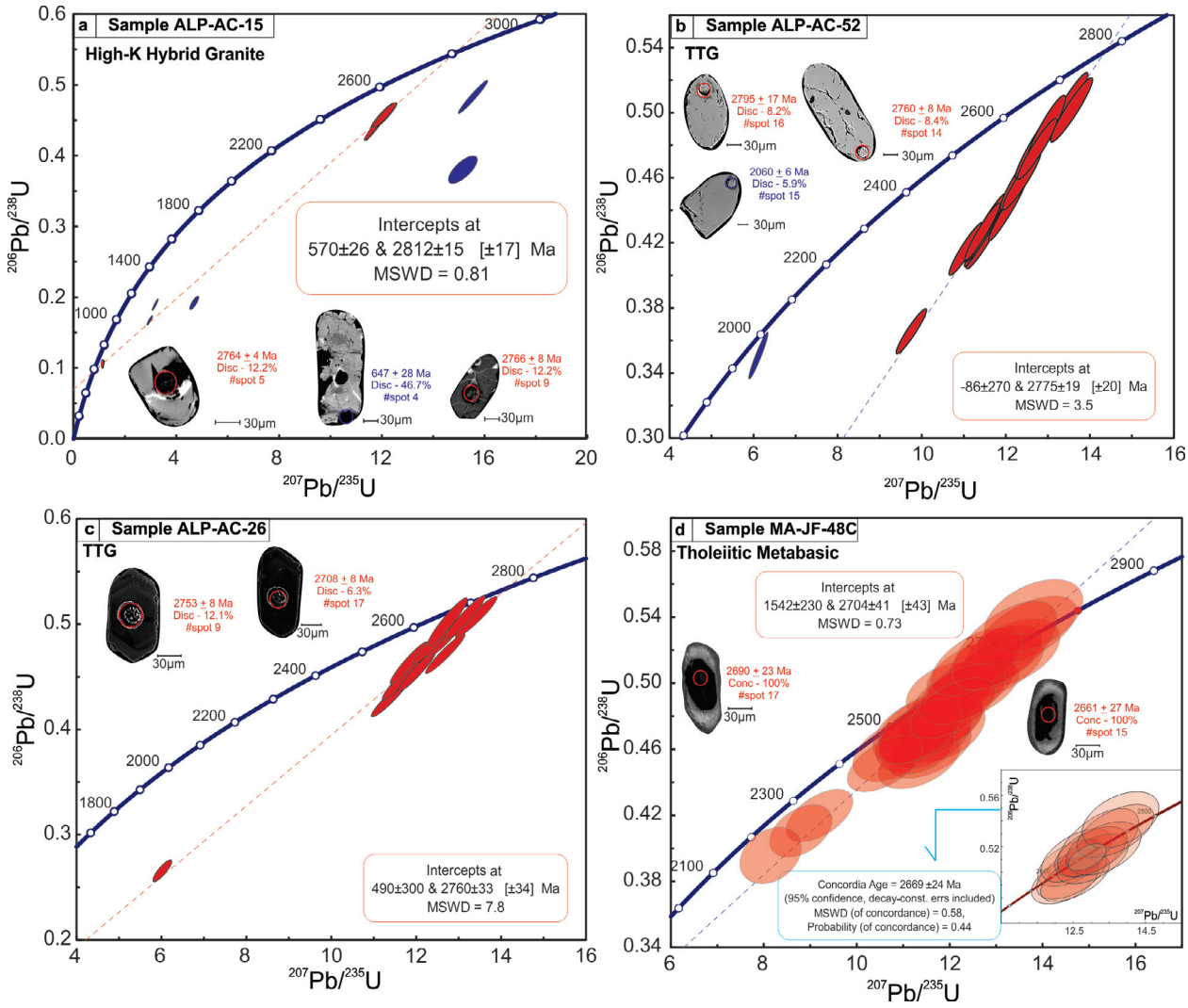

Fig. 10. LA-ICPMS U–Pb concordia diagrams of the selected rocks of the Campos Gerais complex in the target areas: (a) High-K hybrid granite II (ALP-AC-15); (b) late intrusive TTG tonalite (ALP-AC-52); (c) late intrusive TTG tonalite (ALP-AC-26); (d) within-plate tholeiitic metabasic amphibolite (MA-JF-48C).

4.4.5. Intrusive TTG tonalites (samples ALP-AC-52 and ALP-AC-26)

Sample ALP-AC-52 is a non-foliated intrusive hornblende-tonalite of TTG affinity. It has short, prismatic pink zircons, 20 of which were analyzed. Sixteen grains define a discordia line yielding an upper intercept age of 2775 ± 19 Ma (MSWS = 3.5) (Fig. 10b). One analysis located in a zone of new growth domain yielded a $^{207}Pb/^{206}Pb$ age of 2060 ± 6 Ma (5.9% discordant).

Sample ALP-AC-26 has the same field and petrographic characteristics as the previous sample. Zircon grains are typically euhedral, colorless to pale pink crystals. Fifteen grains define a discordia line yielding an upper intercept age of 2760 ± 33 Ma (MSWD = 7.8) (Fig. 10c), which coincides well with that of sample ALP-AC-52, despite the high MSWD.

4.4.6. Amphibolite (sample MA-JF-48C)

Sample MA-JF-48C is a tholeiitic amphibolite with within-plate N-MORB geochemical characteristics from the Minduri inlier. This sample has prismatic, euhedral to subhedral zircon grains varying from light to dark brown in colour with fine igneous oscillatory zoning. Thirty-five analyses define a discordia line yielding with an upper intercept age of 2704 ± 41 Ma (MSWD = 0.73) and a lower intercept age at 1542 ± 230 Ma (Fig. 10d). Eleven data points yield a concordia age of 2669 ± 24 Ma (MSWD = 0.58) which is interpreted as the crystallization age of the rock.

4.5. Zircon Lu–Hf isotopes

Eleven nearly concordant (>90%) zircon grains from the Neoarchean sanukitoid sample MA-JF-49B were chosen for Lu–Hf analysis (Supplementary Data E). Two of the analyzed concordant grains show $^{207}Pb/^{206}Pb$ ages of ca. 2.76 Ga and 2.78 Ga, which are much younger than that of the crystallization age of the rock (2910 ± 19 Ma). Since they yielded $^{176}Hf/^{177}Hf_{(t)}$ in the same range of the other grains, their ages were interpreted as resulting from Pb loss. It may be geologically significant that their ages are coincident with the late TTG magmatism (Fig. 12), which may have disturbed the U–Pb system. The range of initial ε_{Hf} varies from − 1.69 to + 3.31, suggesting juvenile magmatism, i.e., derived from melting of mantle rocks. Initial $^{176}Hf/^{177}Hf$ varies from 0.28087 ± 0.00005 to 0.28093 ± 0.00005, and depleted-mantle Hf model ages (T_{DM}) vary from 3.12 Ga to 3.42 Ga. The petrogenetic implications of the Hf isotope data are discussed below.

4.6. Whole-rock Sm–Nd isotopes

New Sm–Nd isotope analyses were obtained from a Neoarchean sanukitoid (sample MA-JF-49B) and a within-plate tholeiitic metabasic amphibolite (sample MA-JF-48C). Major and trace element data are shown in Table 1. The sanukitoid orthogneiss has

Table 1
Analytical data of new Sm–Nd data for tholeiitic metabasic rocks (amphibolites). Age refers to U–Pb crystallization ages of the igneous protoliths. T_{DM} model ages were calculated using the depleted mantle model of DePaolo (1981).

Sample	Rock	Age (Ma)	Sm (ppm)	Nd (ppm)	$^{147}Sm/^{144}Nd$	$^{143}Nd/^{144}Nd$ ±2s st error	$^{143}Nd/^{144}Nd_{(t)}$	$\varepsilon_{Nd}(t)$	T_{DM} (Ga)
MA-JF-49B	Sanukitoid orthogneiss	2891 ± 19	9.5	48.1	0.1196	0.511072 ± 0.000004	0.5088	−1.9	3.02
MA-JF-48C	N-MORB amphibolite	2669 ± 24	3.7	22.5	0.1009	0.510791 ± 0.000004	0.5090	−3.1	2.87

near-chondritic initial ε_{Nd} of − 1.9 (at 2.89 Ga), and T_{DM} model age of 3.02 Ga. The 2.67 Ga tholeiitic within-plate amphibolite has also slightly negative $\varepsilon_{Nd}(t)$ of − 3.1 and T_{DM} of 2.87 Ga.

5. Discussion

5.1. Synthesis of the crustal evolution of the Campos Gerais complex

The integration of field relationships of geochemically characterized rock units with their Sm–Nd isotope characteristics allows a better interpretation of the U–Pb data and of the petrogenetic characteristics. For instance, T_{DM} Sm–Nd model ages (De Paolo, 1981) may be regarded as a maximum age of crystallization, which help evaluate U–Pb ages of crystallization. Initial ε_{Nd} values are useful in assessing the juvenile nature of an igneous rock, whether it is derived from the mantle (positive or slightly negative $\varepsilon_{Nd}(t)$) or from crustal sources. The chronological sequence of dated magmatic events and their corresponding geochemical and isotopic characteristics (Table 2) can be used to outline the temporal Archean crustal evolution of the southwestern region of the São Francisco craton.

Sample ALP-AC-17B is a high-K granite most likely derived from crustal melting due to its peraluminous affinity. Although poorly constrained by the U–Pb data, the crystallization age is most likely between ca. 2.9 Ga ($^{207}Pb/^{206}Pb$ age of youngest magmatic zircon) and 3.13 Ga, which is the T_{DM} Nd model age. As observed in other studied samples below, older zircons with $^{207}Pb/^{206}Pb$ ages from 3.20 Ga to 3.56 Ga are interpreted as inherited. Although most of these grains are highly discordant, their $^{207}Pb/^{206}Pb$ ages are regarded as minimum ages of crystallization, suggesting crustal melting and generation of peraluminous magmas through reworking of Paleoarchean crust.

A subduction-collision tectonic cycle can be outlined, with TTG magmatism represented by predominant trondhjemites and tonalites, represented by sample ALP-AC-37A, with a crystallization age of 2959 ± 5 Ma. The older T_{DM} of 3.24 Ga, the more negative initial ε_{Nd} of − 4.9 and inherited zircons of ca. 3.13 Ga and 3.27 Ga are all indicative of contamination of mantle-derived magmas by older continental crust. Although represented by a single studied sample (MA-JF-49B), the 2.89 Ga sanukitoid orthogneiss has a T_{DM} of 3.02 Ga and primitive $\varepsilon_{Nd}(t)$ of − 1.9. These results are also indicative of generation from partial melting of metasomatized mantle with minimal crustal contamination. This interpretation is corroborated by the range of depleted-like $\varepsilon_{Hf}(t)$ (−1.9 to + 2.98) for concordant zircons from this sample.

The geochemical signatures of TTG rocks and the sanukitoid sample in the primitive mantle-normalized multi-element diagrams of Fig. 8 show the negative Nb, P and Ti anomalies, which are deemed typical of Phanerozoic magmatic arcs (Pearce, 1982). In such case, a cordilleran style of subduction instead of an intra-oceanic one would be favoured by the occurrence of inherited zircon grains and Nd T_{DM} ages slightly older than the interpreted U–Pb crystallization ages, indicating that juvenile magmas were contaminated by older continental crust during their ascent and emplacement.

The development of supracrustal successions represented by the Pitangui and Fortaleza de Minas greenstone belts (Fig. 2), approximately coeval (ca. 2.86 Ga) with the TTG-sanukitoid complexes, suggest an analogy with back-arc basins and magmatic arcs, respectively, in a subduction-like geodynamic setting (Verma et al., 2017).

Convergence and accretion of the magmatic arcs at ca. 2.81–2.82 Ga, leading to the amalgamation of larger continental masses, is indicated by widespread migmatization and generation of high-K granites. These are characterized by either peraluminous affinity, resulting from melting of continental crust, or by a hybrid composition resulting from the involvement of juvenile magmas (Laurent et al., 2014). Sample ALP-AC-19B is a muscovite-bearing peraluminous granite with an interpreted crystallization age of 2810 ± 69 Ma, a much older T_{DM} of 3.57 Ga and more negative initial ε_{Nd} of − 8.1, indications of reworking of older crust. The same characteristics apply to sample ALP-AC-15, a high-K hybrid granite with a similar crystallization age of 2812 ± 15 Ma, T_{DM} of 3.34 Ga and initial ε_{Nd} of − 8.3. Additionally, both samples contain older, Meso- to Paleoarchean inherited zircon grains, with $^{207}Pb/^{206}Pb$ ages respectively of ca. 3.26 Ga and 3.62 Ga, and of 3.08 Ga and 3.41 Ga, which also points to crustal reworking of Meso- to Paleoarchean older crust.

Younger TTG magmatism took place with the intrusion of several tonalite stocks (Fig. 2) at relatively shallow crustal levels of emplacement suggested by their characteristically porphyritic textures and fine-grained matrix. Tonalite samples ALP-AC-52 and ALP-AC-26 yield U–Pb discordia lines with upper intercepts respec-

Table 2
Summary of geochemical affinity, crystallization age, age of inherited zircons, T_{DM} and initial ε_{Nd} for representative rock samples from the Campos Gerais complex, in order of interpreted crystallization age. See text for discussion.

Sample	Compositional group	Crystallization age (Ma)	$^{206}Pb/^{207}Pb$ ages of inherited zircons (Ga)	T_{DM} (Ga)	$\varepsilon_{Nd}(t)$
ALP-AC-17B	High-K hybrid granite	≥ 2912 ± 16	3.20–3.56	3.13	−3.8
ALP-AC-37A	TTG orthogneiss	2959 ± 5	3.27 3.13	3.24	−4.9
MA-JF-49B	Sanukitoid tonalite	2891 ± 19	–	3.02	−1.9
ALP-AC-19B	High-K peraluminous granite	2820 ± 69	3.62 3.26	3.57	−8.1
ALP-AC-15	High-K hybrid granite	2812 ± 15	3.41 3.08	3.34	−8.6
ALP-AC-52	Late TTG tonalite	2775 ± 19	–	2.80	−0.1
ALP-AC-26	Late TTG tonalite	2760 ± 33	–	2.88	−1.5
MA-JF-48C	Tholeiitic amphibolite	2669 ± 24	–	2.87	−3.1

tively of 2775 ± 19 Ma and 2760 ± 33 Ma. Although both discordia present poor regressions, resulting in rather high MSWD of 3.3 and 7.8, the two dates can be regarded as having geological meaning, and are interpreted as crystallization ages. Collected from two different intrusive stocks, the two samples yielded overlapping ages (given their associated uncertainties) which are compatible with their late intrusive character, as observed in the field. Near-chondritic initial ε_{Nd} values (−0.1 and − 1.5) and absence of inherited zircons are indicative of their juvenile character without any significant crustal contamination. This younger TTG magmatism might be related to renewed subduction-like processes along the continental margin, with shallow melting of basaltic sources at low pressures, according to the criteria defined by Halla (2005), Martin et al. (2009), and Halla et al. (2009).

Following the emplacement of the ca. 2.77 Ga post-collisional tonalites, crustal cooling and stabilization of the amalgamated continental crust allowed the emplacement at 2.67 Ga of within-plate tholeiitic mafic rocks (amphibolite sample MA-JF-48C). Within-plate magmatic episodes during the latest Neoarchean are likely associated with the early extensional regimes that eventually led to the ca. 2.5 Ga continental rifting and the Paleoproterozoic Wilson cycle represented by the Minas Supergroup rift-drift-foreland basin. The Minas sedimentary basin was inverted during the development of the Rhyacian orogenic processes between 2.10 Ga and 2.05 Ga, which reworked the southernmost portion of the SFC (Machado et al., 1996a; Martinez-Dopico et al., 2017; Moreira et al., 2018; Cutts et al., 2020; Rossignol et al., 2020). An indication that the latter orogeny could have affected the CGC is provided by zircon cores surrounded by new growth rims with $^{207}Pb/^{206}Pb$ ages of 2060 ± 6 Ma (sample ALP-AC-17B) and of 2075 ± 4 Ma (sample ALP-AC-52).

5.2. Correlations with other Archean blocks in the southern São Francisco craton

Fig. 11 depicts a summary of age constraints for the main tectonic processes in the CGC, compared with those of other Archean granite-greenstone crustal blocks and sectors of the southern SFC. The latter include the Campo Belo complex, Pitangui greenstone-belt area and Iron Quadrangle sector, and the *para*-autochthonous Piumhi sliver (Brasilia belt) and the Piedade complex (Ribeira belt). A highly diachronous picture arises, with several sectors showing protracted subduction-like periods, represented by magmatic arc products such as TTG and sanukitoid orthogneisses, punctuated by short-lived collisional events indicated by high-K, frequently peraluminous granites. The oldest records of TTG production are around 3.2 Ga, recorded in the Campo Belo and Santa Bárbara complexes (Teixeira et al., 1996; Lana et al., 2013). TTG magmatism at ca. 2.9 Ga, such as described here in the CGC was also described in the parautochthonous Piumhi granite-gneiss sliver (Valeriano et al., 2004). However, the 2.89 Ga sanukitoid rock described in the CGC has until now only been reported in an Archean inlier within the Mineiro belt (Simon et al., 2018), which was not accreted against the southern São Francisco craton until 2.10 Ga. Younger Archean sanukitoid rocks of ca. 2.67 Ga were also described in the Piedade microcontinent farther south, which was accreted at 2.05 Ga (Bruno et al., 2020).

Paleoarchean inherited zircon grains are recorded in the TTG orthogneisses of most sectors of southern SFC. Older inherited zircon grains associated with the $^{207}Pb/^{207}Pb$ age between 3.4 Ga and 3.62 Ga occur only in the CGC and are regarded as vestiges of Paleo- to Eoarchean crust in this sector of the SFC.

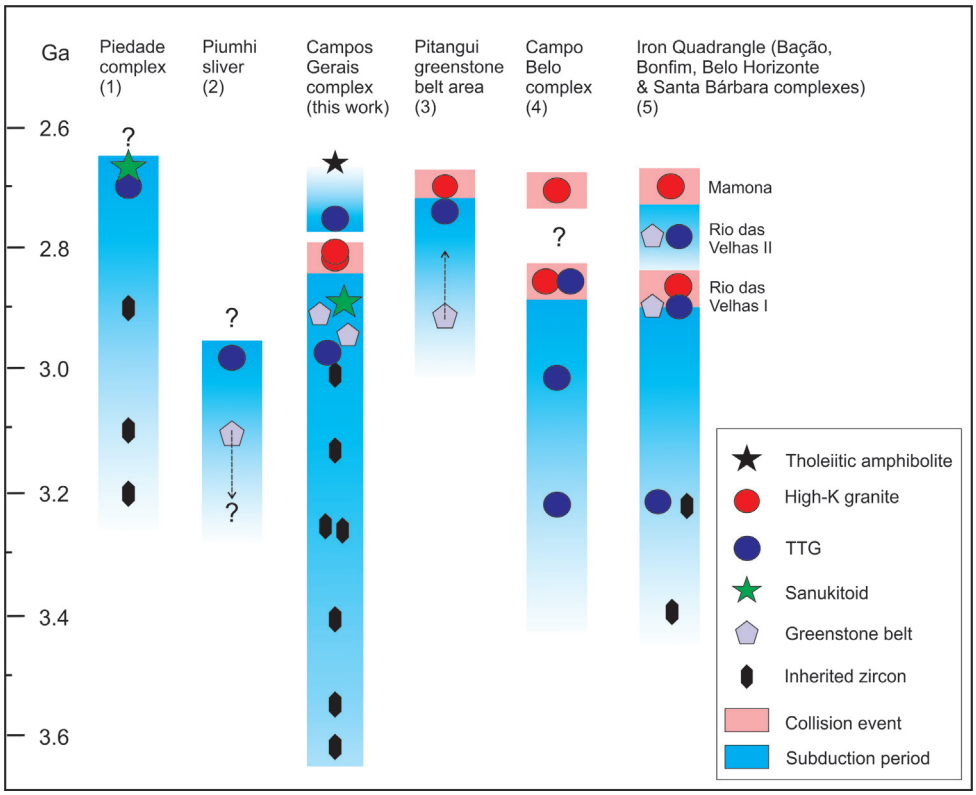

Fig. 11. Comparative Archean tectonic evolution of the different sectors of the southern São Francisco craton. Data from: (1) Bruno et al., 2020, 2021; (2) Valeriano et al., 2004; (3) Soares et al., 2020; (4) Teixeira et al., 1996; (5) Lana et al., 2013; Farina et al., 2015; Albert et al., 2016.

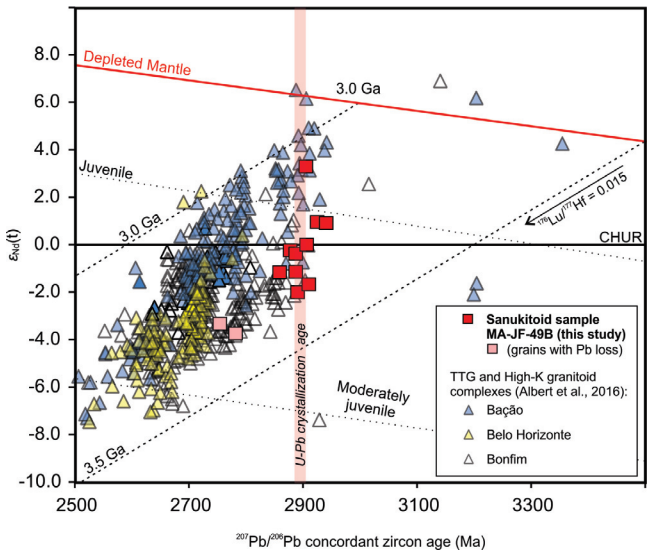

Fig. 12. Lu–Hf zircon data for Archean rocks from Bação, Belo Horizonte and Santa Bárbara complexes, in the Iron Quadrangle sector of the southern São Francisco craton (data from Albert et al., 2016). Red squares represent new data for the 2.89 Ga sanukitoid tonalite sample (MA-JF-49B) from the Campos Gerais Complex, the oldest yet recorded in the São Francisco craton.

Collisional events are diachronous, but two main episodes are recorded: an older set of events at ca. 2.85 Ga and 2.82 Ga respectively in the Iron Quadrangle and CGC, referred as Rio das Velhas I (Farina et al., 2016), and another event at ca. 2.7 Ga, the Mamona event, also present in the Pitangui greenstone belt and in the Campo Belo complex. The Mamona event was not recorded in the CGC, which may have been tectonically stable by 2.67 Ga, when within-plate tholeiitic magmatism preceded the ca. 2.6 Ga Minas continental rifting (Rossignol et al., 2020).

The existence of distinct tectono-stratigraphic terranes with different crustal evolution histories in the southern SFC is also suggested by the ε_{Hf} vs. $^{207}Pb/^{206}Pb$ age diagram (Fig. 12) from the Bação, Belo Horizonte and Bonfim complexes of the Iron Quadrangle area (Albert et al., 2016). The Archean crust of the southern SFC seems to represent the amalgamation of different microcontinental blocks that occurred during the several collisional episodes represented by the 2.85 Ga (Campo Belo complex and Iron Quadrangle), 2.82 Ga (CGC) and 2.70 Ga (Pitangui greenstone belt area, Campo Belo complex and Iron Quadrangle area) high-K leucogranites.

6. Conclusions

The characterization of Mesoarchean continental crust in the southwestern periphery of the SFC adds important information to the reconstruction of Archean nuclei that were assembled during the Rhyacian orogeny.

The Archean crustal evolution recorded in the CGC complex can be briefly summarized as follows. The 2.96 Ga TTG and 2.89 Ga sanukitoid magmatic rocks represent continental magmatic arcs with variable crustal contamination resulting from subduction-like processes of oceanic slabs along a Meso- to Paleoarchean continental margin. A collisional event at ca. 2.82–2.81 Ga resulted in the migmatization of the previous rock association, with the emplacement of high-K leucogranites. Renewed 2.77–2.76 Ga intrusive tonalitic TTG magmatism may be indicative of a new phase of subduction-like processes. Within-plate 2.67 Ga tholeiitic mafic magmatism completes the Archean evolution preceding the onset of Paleoproterozoic rifting and later processes.

Finally, the CGC contains evidence for significant differences in the timing of major tectonic events compared to other Archean terrains in the southern São Francisco craton, including an independent Meso- to Neoarchean crustal evolution. This is consistent with models for Archean crustal evolution that involve the semi-independent development of a larger number of relatively small microcontinents that were progressively amalgamated as result of collision at subduction zones.

Declaration of Competing Interest

The authors declare that they have no known competing financial interests or personal relationships that could have appeared to influence the work reported in this paper.

Acknowledgements

This work was carried out with support from the PRONAGEO mapping program of the CPRM (Brazilian Geological Service). CNPq and FAPERJ contributed with funding to CMV and MH respectively. The authors are grateful to the following persons: Apoena Rossi for invaluable help during field work; Joseph Dunlop and Geoff Long from University of Portsmouth for lab support. CMV and MH acknowledge CNPq and HB for FAPERJ scholarships. F. Farina and an anonymous reviewer contributed with important comments which improved an earlier version of the manuscript.

Appendix A. Supplementary data

Supplementary data to this article can be found online at https://doi.org/10.1016/j.gsf.2022.101372.

References

Albert, C., Farina, F., Lana, C., Stevens, G., Storey, C., Gerdes, A., Dopico, C.M., 2016. Archean crustal evolution in the Southern São Francisco craton, Brazil: Constraints from U-Pb, Lu-Hf and O isotope analyses. Lithos 266-267, 64–86.

Alkmim, F.F., Teixeira, W., 2017. Chapter 5: The Paleoproterozoic Mineiro belt and the Quadrilatero Ferrífero. In: Heilbron, M., Alkmim, F., Cordani, U.G. (Eds.), The São Francisco Craton and its Margins, Eastern Brazil. Regional Geology Review Series. Springer Verlag, pp. 71–94.

Barbosa, J.S.F., Barbosa, R.G., 2017. Chapter 4: The Paleoproterozoic Eastern Bahia orogenic domain. In: Heilbron, M., Alkmim, F., Cordani, U.G. (Eds.), The São Francisco Craton and its Margins, Eastern Brazil. Regional Geology Review Series. Springer Verlag, pp. 57–70.

Barbosa, N.d.S., Teixeira, W., Leal, L.R.B., Leal, A.B.d.M., 2013. Evolução crustal do setor Ocidental do Bloco Arqueano Gavião, Cráton do São Francisco, com base em evidências U-Pb, Sm-Nd e Rb-Sr. Rev. Geol. USP. Série Cient. 13 (4), 63–88 (in Portuguese).

Barbosa, N., Menezes Leal, A.B., Debruyne, D., Bastos Leal, L.R., Barbosa, N.S., Marinho, M., Mercês, L., Barbosa, J.S., Koproski, L.M., 2020. Paleoarchean to Paleoproterozoic crustal evolution in the Guanambi Correntina block (GCB), north São Francisco Craton, Brazil, unraveled by UPb Geochronology, Nd-Sr isotopes and geochemical constraints. Precambr. Res. 340, 105614. https://doi.org/10.1016/j.precamres.2020.105614.

Bastos Leal, L.R., Cunha, J.C., Cordani, U.G., Teixeira, W., Nutman, A.P., Menezes Leal, A.B., Macambira, M.J.B., 2003. SHRIMP U-Pb, $^{207}Pb/^{206}Pb$ zircon dating, and Nd isotopic signature of the Umburanas Greenstone Belt, northern São Francisco Craton. Brazil. J. S. Am. Earth Sci. 15 (7), 775–785.

Bédard, J.H., 2006. A catalytic delamination-driven model for coupled genesis of Archaean crust and sub-continental lithospheric mantle. Geochem. Cosmochim. Acta 70 (5), 1188–1214.

Bédard, J.H., 2018. Stagnant lids and mantle overturns: implications for Archaean tectonics, magmagenesis, crustal growth, mantle evolution, and the start of plate tectonics. Geosci. Front. 9 (1), 19–49.

Bersan, S.M., Danderfer Filho, A., Abreu, F.R.d., Lana, C., 2018. Petrography, geochemistry and geochronology of the potassic granitoids of the Rio Itacambiruçu supersuite: implications for the Meso- to Neoarchean evolution of the Itacambira-Monte Azul block. Braz. J. Geol. 48 (1), 1–24.

Boynton, W.V., 1984. Geochemistry of the rare earth elements: meteorite studies. In: Henderson, P. (Ed.), Rare-earth Element Geochemistry. Elsevier, pp. 63–114.

Bruno, H., Elizeu, V., Heilbron, M., de Morisson Valeriano, C., Strachan, R., Fowler, M., Bersan, S., Moreira, H., Dussin, I., Guilherme do Eirado Silva, L., Tupinambá, M., Almeida, J., Neto, C., Storey, C., 2020. Neoarchean and Rhyacian TTG-Sanukitoid suites in the southern São Francisco Paleocontinent, Brazil: Evidence for

diachronous change towards modern tectonics. Geosc. Front. 11 (5), 1763–1787.
Bruno, H., Heilbron, M., de Morisson Valeriano, C., Strachan, R., Fowler, M., Bersan, S., Moreira, H., Motta, R., Almeida, J., Almeida, R., Carvalho, M., Storey, C., 2021. Evidence for a complex accretionary history preceding the amalgamation of Columbia: The Rhyacian Minas-Bahia Orogen, southern São Francisco Paleocontinent, Brazil. Gondwana Res. 92, 149–171.
Campos, J.C.S., Carneiro, M.A., Basei, M.A.S., 2003. U-Pb evidence for Neoarchean crustal reworking in southern São Francisco Craton (Minas Gerais, Brazil). Anais da Academia Brasileira de Ciências 75, 497–511.
Campos Neto, M.C., 2000. Orogenic Systems from southwestern Gondwana: an approach to Brasiliano-Pan African Cycle and orogenic collage in southeastern Brazil. In: Cordani, U.G., Milani, E.J., Thomaz Filho, A., Campos, D.A. (Eds.), Tectonic Evolution of South America. 31th Intern. Geol. Congr. Rio de Janeiro, Brazil, 335–365.
Carneiro, M.A., Teixeira, W., Carvalho Junior, I.M., Fernandes, R.A., 1998. Ensialic tectonic setting of the Archean Rio das Velhas greenstone belt: Nd and Pb isotopic evidence from the Bonfim Metamorphic Complex, Quadrilátero Ferrífero, Brazil. Revista Brasileira de Geociências 28, 189–200.
Cioffi, C.R., Campos Neto, M.C., Möller, A., Rocha, B.C., 2016. Paleoproterozoic continental crust generation events at 2.15 and 2.08 Ga in the basement of the southern Brasília Orogen, SE Brazil. Precambr. Res. 275, 176–196.
Corfu, F., Hanchar, J.M., Hiskin, P.W.O., Kinny, P., 2003. Atlas of zircon textures. Rev. Miner. Geochem. 53, 469–500.
Cox, K.G., Bell, J.D., Pankhurst, R.J., 1979. The Interpretation of Igneous Rocks. Allen & Unwin, London, p. 450.
Cruz, S.C.P., Peucat, J.-J., Teixeira, L., Carneiro, M.A., Marques Martins, A.A., Santana, J.D.S., de Souza, J.S., Barbosa, J.S.F., Leal, Â.B.M., Dantas, E., Pimentel, M., 2012. The Caraguataí syenitic suite, a ca. 2.7 Ga-old alkaline magmatism (petrology, geochemistry and U-Pb zircon ages) Southern Gavião block (São Francisco Craton). Brazil. J. S. Am. Earth Sci. 37, 95–112.
Cutts, K., Lana, C., Moreira, H., Alkmim, F., Peres, G.G., 2020. Zircon U-Pb and Lu-Hf recordfrom high-grade complexes within the Mantiqueira complex: first evidence of juvenile crustal input at 2.4–2.2 Ga and implications for the Palaeoproterozoic evolution of the São Francisco Craton. Precambr. Res. 338, 105567. https://doi.org/10.1016/j.precamres.2019.105567.
Dantas, E.L., Souza, Z.S., Wernick, E., Hackspacher, P.C., Martin, H., Xiaodong, D., Li, J. W., 2013. Crustal growth in the 3.4–2.7 Ga Sao Jose de Campestre Massif, Borborema Province. NE Brazil. Precambrian Res. 227, 120–156.
Degler, R., Pedrosa-Soares, A., Novo, T., Tedeschi, M., Silva, L.C., Dussin, I., Lana, C., 2018. Rhyacian-Orosirian isotopic records from the basement of the Araçuaí-Ribeira orogenic system (SE Brazil): links in the Congo-São Francisco palaeocontinent. Precambr. Res. 317, 179–195.
De Paolo, D.J., 1981. Neodymium isotopes in the Colorado Front Range and crustal mantle evolution in the Proterozoic. Nature 291, 193–197.
Farina, F., Albert, C., Lana, C., 2015. The Neoarchean transition between medium- and high-K granitoids: Clues from the Southern São Francisco Craton (Brazil). Precambr. Res. 266, 375–394.
Farina, F., Albert, C., Martínez Dopico, C., Aguilar Gil, C., Moreira, H., Hippertt, J.P., Cutts, K., Alkmim, F.F., Lana, C., 2016. The Archean-Paleoproterozoic evolution of the Quadrilátero Ferrífero (Brasil): current models and open questions. J. S. Am. Earth Sci. 68, 4–21.
François, C., Philippot, P., Rey, P., Rubatto, D., 2014. Burial and exhumation during Archean sagduction in the East Pilbara Granite-Greenstone Terrane. Earth and Planet. Sci. Lett. 396, 235–251.
Frost, B.R., Barnes, C.G., Collins, W.J., Arculus, R.J., Ellis, D.J., Frost, C.D., 2001. A geochemical classification for granitic rocks. J. Petrol. 42, 2033–2048.
Gerya, T., 2014. Precambrian geodynamics: Concepts and models. Gondwana Res. 25, 442–463.
Halla, J., 2005. Late Archean high-Mg granitoids (sanukitoids) in the southern Karelian domain, eastern Finland: Pb and Nd isotopic constraints on crust-mantle interactions. Lithos 79 (1-2), 161–178.
Halla, J., van Hunen, J., Heilimo, E., Hölttä, P., 2009. Geochemical and numerical constraints on Neoarchaean plate tectonics. Precambr. Res. 174, 155–162.
Hartmann, L.A., Endo, I., Suita, M.T.F., Santos, J.O.S., Frantz, J.C., Carneiro, M.A., McNaughton, N.J., Barley, M.E., 2006. Provenance and age delimitation of Quadrilátero Ferrífero sandstones based on zircon U-Pb isotopes. J. S. Am. Earth Sci. 20 (4), 273–285.
Heilbron, M., Ribeiro, A., Valeriano, C.M., Paciullo, F.V., Almeida, J.C.H., Trouw, R.J.A., Tupinambá, M., Eirado, L.G., Cordani, U.G., 2017. The Ribeira Belt. In: Heilbron, M., Alkmim, F., Cordani U. (Eds.), The São Francisco Craton and its Margins, Eastern Brazil. Regional Geology Review Series. Springer-Verlag, Chapter 15, pp. 277–302.
Heilimo, E., Halla, J., Hölttä, P., 2010. Discrimination and origin of the sanukitoid series: Geochemical constraints from the Neoarchean western Karelian Province (Finland). Lithos 115 (1-4), 27–39.
Jiang, N., Guo, J., Fan, W., Hu, J., Zong, K., Zhang, S., 2016. Archean TTGs and sanukitoids from the Jiaobei terrain, North China craton: insights into crustal growth and mantle metasomatism. Precambr. Res. 281, 656–672.
Lana, C., Alkmim, F.F., Armstrong, R., Scholz, R., Romano, R., Nalini, H.A., 2013. The ancestry and magmatic evolution of Archaean TTG rocks of the Quadrilátero Ferrífero province, southeast Brazil. Precambr. Res. 231, 157–173.
Larionova, Y.O., Samsonov, A.V., Shatagin, K.N., 2007. Sources of Archean sanukitoids (High-Mg subalkaline granitoids) in the Karelian craton: Sm-Nd and Rb-Sr isotopic-geochemical evidence. Petrology 15 (6), 530–550.
Laurent, O., Martin, H., Moyen, J.F., Doucelance, R., 2014. The diversity and evolution of late Archean granitoids: evidence for the onset of 'modern-style' plate tectonics between 3.0 and 2.5 Ga. Lithos 205, 208–235.
Machado, N., Noce, C.M., Ladeira, E.A., Oliveira, O.B., 1992. U-Pb geochronology of Archean magmatism and Proterozoic metamorphism in the Quadrilátero Ferrífero, southern São Francisco Craton, Brazil. Geol. Soc. Am. Bull. 104, 1221–1227.
Machado, N., Valladares, C., Heilbron, M., Valeriano, C., 1996a. U-Pb geochronology of the central Ribeira Belt (Brazil) and implications for the evolution of the Brazilian Orogeny. Precambr. Res. 79 (3-4), 347–361.
Machado, N., Schrank, A., 1989. Geocronologia U–Pb no maciço de Piumhi—resultados preliminares. In: Simposio de Geologia de Minas Gerais 5, Belo Horizonte. Anais. SBG. Núcleo Minas Gerais, Bol., 45–49
Machado, N., Schrank, A., Noce, C.M., Gauthier, G., 1996b. Ages of detrital zircon from Archean-Paleoproterozoic sequences: Implications for Greenstone Belt setting and evolution of a Transamazonian foreland basin in Quadrilátero Ferrífero, southeast Brazil. Earth Planet. Sci. Lett. 141 (1-4), 259–276.
Martin, H., 1986. Effect of steeper Archean geothermal gradient on geochemistry of subduction-zone magmas. Geology 14 (9), 753. https://doi.org/10.1130/0091-7613(1986)14<753:EOSAGG>2.0.CO;2.
Martin, H., Peucat, J.J., Sabaté, P., Cunha, J.C., 1997. Crustal evolution in early Archean of South America: example of Sete Voltas massif, Bahia state. Brazil. Precambrian Res. 82, 35–62.
Martin, H., Moyen, J.-F., Rapp, R., 2009. The sanukitoid series: magmatism at the Archaean-Proterozoic transitions. Trans. R. Soc. Edinb. Earth Sci. 100 (1-2), 15–33.
Martínez Dopico, C.I., Lana, C., Moreira, H.S., Cassino, L.F., Alkmim, F.F., 2017. U-Pb ages and Hf-isotope data of detrital zircons from the late Neoarchean-Paleoproterozoic Minas Basin. SE Brazil. Precambrian Res. 291, 143–161.
McDonough, W.F., Sun, S.-s., 1995. The composition of the Earth. Chem. Geol. 120 (3-4), 223–253.
Moreira, H., Lana, C., Nalini, H.A., 2016. The detrital zircon record of an Archaean convergent basin in the Southern São Francisco Craton. Brazil. Geosc. Front. 275, 84–99.
Moreira, H., Seixas, L., Storey, C., Fowler, M., Lasalle, S., Stevenson, R., Lana, C., 2018. Evolution of Siderian juvenile crust to Rhyacian high Ba-Sr magmatism in the Mineiro Belt, southern São Francisco Craton. Precambr. Res. 9 (4), 977–995.
Moyen, J.F., Laurent, O., 2018. Archean tectonic systems? A view from igneous rocks. Lithos 302–303, 99–125.
Mulder, J.A., Nebel, O., Gardiner, N.J., Cawood, P.A., Winwright, A.N., Ivanic, T.J., 2021. Crustal rejuvenation stabilised Earth's first cratons. Nature Comm. 12, 3535.
Noce, C.MAURÍCIO., Machado, NUNO, Teixeira, WILSON, 1998. U-Pb geochronology of gneisses and granitoids in the Quadrilátero Ferrífero (Southern São Francisco Craton): age constraints for Archean and Paleoproterozoic magmatism and metamorphism. Rev. Bras. Geoc. 28 (1), 95–102.
Noce, C., Zuccheti, M., Baltazar, O., Armstrong, R., Dantas, E., Renger, F., Lobato, L., 2005. Age of felsic volcanism and the role of ancient continental crust in the evolution of the Neoarchean Rio das Velhas greenstone belt (Quadrilátero Ferrífero, Brazil): U-Pb zircon dating of volcaniclastic graywackes. Precambr. Res. 141 (1-2), 67–82.
Nutman, A.P., Cordani, U.G., 1993. SHRIMP U-Pb zircon geochronology of Archaean granitoids from the Contendas-Mirante area of the São Francisco Craton, Bahia, Brazil. Precambr. Res. 63 (3-4), 179–188.
O'Connor, J.T., 1965. A classification for quartz-rich igneous rocks based on feldspar ratios. USGS Prof. Pap. 525-B, B79–B84.
Oliveira, E.P., McNaughton, N.J., Armstrong, R., 2010. Mesoarchaean to Palaeoproterozoic growth of the northern segment of the Itabuna–Salvador–Curaçá orogen, São Francisco craton, Brazil. Geological Society, London, Special Publications 338 (1), 263–286.
Oliveira, E.P., McNaughton, N.J., Zincone, S.A., Talavera, C., 2020. Birthplace of the São Francisco Craton, Brazil: Evidence from 3.60 to 3.64 Ga Gneisses of the Mairi Gneiss Complex. Terra Nova 32, 281–289.
Paquette, J.L., Barbosa, J.S.F., Rohais, S., Cruz, S.C.P., Goncalves, P., Peucat, J.J., Leal, A. B.M., Santos-Pinto, M., Martin, H., 2015. The geological roots of South America: 4.1 Ga and 3.7 Ga zircon crystals discovered in N.E. Brazil and N.W. Argentina. Precambr. Res. 271, 49–55.
Pearce, J.A., 1982. Trace element characteristics of lavas from destructive plate boundaries. In: Thorpe, R.S. (Ed.), Andesites. John Wiley & Sons, pp. 525–548.
Peccerillo, A., Taylor, S.R., 1976. Geochemistry of Eocene calc-alkaline volcanic rocks from the Kastamonu area, Northern Turkey. Contrib. Min. Petrol. 58 (1), 63–81.
Peucat, J.J., Santos Pinto, M., Martin, H., Barbosa, J.S., Fanning, M.C., 2003. SHRIMP U/Pb zircon ages up to 3.4–3.5 Ga in Archean and Paleoproterozoic granitoids of the Gavião Block, São Francisco Craton, Bahia, Brazil. IV South Am. Symp. Isotope Geol., Salvador. Short Papers, 252–255.
Piaia, P., Oliveira, E.P., Valeriano, C.M., 2017. The 2.58 Ga Sao José do Jacuipe gabbro-anorthosite stratiform complex, Itabuna-Salvador-Curaçá Orogen, São Francisco Craton, Brazil: Root of the Neoarchaean Caraiba continental arc? J. S. Am. Earth Sci. 79, 326–341.
Pimentel, MÁRCIO.M., Ferreira filho, CÉSAR.F., 2002. Idade Sm-Nd de komatiitos do Greenstone belt do Morro do Ferro, Fortaleza de Minas (MG). Rev. Bras. Geoc. 32 (1), 147–148.
Pinheiro, M.A.P., Guice, G.L., Magalhães, J.R., 2021. Archean-Ediacaran evolution of the Campos Gerais Domain — A reworked margin of the São Francisco paleocontinent (SE Brazil): Constraints from metamafic–ultramafic rocks. Geosc. Front., 101201 https://doi.org/10.1016/j.gsf.2021.101201.

C.P. Pinto M.A. Silva Mapa Geológico do Estado de Minas Gerais (Geological Map of Minas Gerais State), Escala 1:1.000.000 2014 Companhia de Desenvolvimento Econômico de Minas Gerais, CODEMIG e Serviço Geológico do Brasil, Belo Horizonte, MG (in Portuguese).

Rajesh, H.M., Belyanin, G.A., Van Reenen, D.D., 2018. Three tier transition of Neoarchean TTG-sanukitoid magmatism in the beit bridge complex, Southern Africa. Lithos 296-299, 431–451.

Roman, A., Arndt, N., 2020. Differentiated Archean oceanic crust: Its thermal structure, mechanical stability and a test of the sagduction hypothesis. Geoch. et Cosmoch. Acta 278, 65–77.

Rossignol, C., Lana, C., Alkmim, F., 2020. Geodynamic evolution of the Minas Basin, southern São Francisco Craton (Brazil), during the early Paleoproterozoic: Climate or tectonic? J. S. Am. Earth Sci. 101, 102628. https://doi.org/10.1016/j.jsames.2020.102628.

Shand, S.J., 1943. Eruptive Rocks. John Wiley, New York, p. 444.

Silva, L.C.d., Pedrosa-Soares, A.C., Armstrong, R., Pinto, C.P., Magalhães, J.T.R., Pinheiro, M.A.P., Santos, G.G., 2016. Disclosing the Paleoarchean to Ediacaran history of the São Francisco craton basement: the Porteirinha domain (northern Araçuaí orogen, Brazil). J. S. Am. Earth Sci. 68, 50–67.

Simon, M.B., Marques Bongiolo, E., Ávila, C.A., Oliveira, E.P., Teixeira, W., Stohler, R. C., Soares de Oliveira, F.V., 2018. Neoarchean reworking of TTG-like crust in the southernmost portion of the São Francisco Craton: U-Pb zircon dating and geochemical evidence from the São Tiago Batholith. Precambr. Res. 314, 353–376.

Smithies, R.H., Lu, Y., Kirkland, C.L., Johnson, T.E., Mole, D.R., Champion, D.C., Martin, L., Jeon, H., Wingate, M.T.D., Johnson, S.P., 2021. Oxygen isotopes trace the origins of Earth's earliest continental crust. Nature 592 (7852), 70–75.

Brando Soares, M., Corrêa Neto, A.V., Fabricio-Silva, W., 2020. The development of a Meso- to Neoarchean rifting-convergence collision-collapse cycle over an ancient thickened protocontinent in the south São Francisco craton. Brazil. Gondwana Res. 77, 40–66.

Teixeira, W., Carneiro, M.A., Noce, C.A., Machado, N., Sato, K., Taylor, P.N., 1996. Pb, Sr and Nd isotope constraints on the Archean evolution of gneissic granitoid complexes in the southern São Francisco Craton. Brazil. Precambrian Res. 78, 151–164.

Teixeira, W., Oliveira, E.P., Marques, L.S., 2017. Nature and Evolution of the Archean Crust of the São Francisco Craton. In: Heilbron, M., Alkmim, F., Cordani, U. (Eds.), São Francisco Craton. Eastern Brazil, Tectonic genealogy of a Miniature Continent. Springer, pp. 29–57.

Trouw, R.A.J., Paciullo, F.V.P., Ribeiro, A., 2002. Geologia da Folha Caxambu, escala de 1:100.000. Mapa geológico e texto explicativo 2002 CODEMIG, Belo Horizonte (in Portuguese).

Trouw, R.A.J., Peternel, R., Ribeiro, A., Heilbron, M., Vinagre, R., Duffles, P., Trouw, C. C., Fontainha, M., Kussama, H.H., 2013. A new interpretation for the interference zone between the southern Brasília belt and the central Ribeira belt, SE Brazil. J. S. Am. Earth Sci. 48, 43–57.

Turbay, C.V.G., Valeriano, C.M., Rossi, A., Rocha e Silva, V.G.M., 2008. Geologia do Complexo Campos Gerais ao sul de Alpinópolis, sudoeste de Minas Gerais. Geonomos 16, 79–90 (in Portuguese).

Turbay, C.V.G., Valeriano, C.M., 2012. Litogeoquímica do Complexo Campos Gerais e granitoides intrusivos, Arqueano/Paleoproterozoico, Brasil. Braz. J. Geol. 42, 663–689 (in Portuguese).

Valeriano, C.M., Machado, N., Simonetti, A., Valladares, C.S., Seer, H.J., Simões, L.S.A., 2004. U-Pb geochronology of the southern Brasília belt (SE-Brazil): sedimentary provenance, Neoproterozoic orogeny and assembly of West Gondwana. Precambr. Res. 130, 27–55.

Verma, S.K., Oliveira, E.P., Silva, P.M., Moreno, J.A., Amaral, W.S., 2017. Geochemistry of komatiites and basalts from the Rio das Velhas and Pitangui greenstone belts, São Francisco Craton, Brazil: Implications for the origin, evolution, and tectonic setting. Lithos 284-285, 560–577.

Wiemer, D., Schrank, C.E., Murphy, D.T., Wenham, L., Allen, C.M., 2018. Earth's oldest stable crust in the Pilbara Craton formed by cyclic gravitational overturns. Nature Geosc. 11 (5), 357–361.

Windley, B.F., Kusky, T., Polat, A., 2021. Onset of plate tectonics by the Eoarchean. Precambr. Res. 352, 105980. https://doi.org/10.1016/j.precamres.2020.105980.

Zincone, S.A., Oliveira, E.P., Ribeiro, B.P., Marinho, M.M., 2020. High-K granites between the Archean Gavião and Jequié blocks, São Francisco Craton, Brazil: Implications for cratonization and amalgamation of the Rhyacian Atlantica continent. J. S. Am. Earth Sci. 105, 102920. https://doi.org/10.1016/j.jsames.2020.102920.